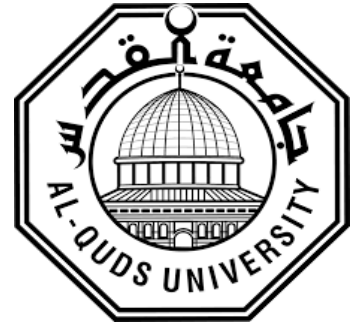


**Deanship of Graduate Studies  
Al-Quds University**



**Influence of Iterative Reconstruction Algorithm on Image  
Quality of Ultra Low-Dose CT Protocol of the Lumbar  
Spine**

**By: Israa Jamal Odeh**

**M.Sc. Thesis**

**Jerusalem- Palestine**

**1444/2022**

Influence of Iterative Reconstruction Algorithm on Image  
Quality of Ultra Low-Dose CT Protocol of the Lumbar  
Spine

Prepared By: Israa Jamal Odeh

B.Sc. of Medical Imaging, Al-Quds University / Palestine

Supervisor: Dr. Hjouj Mohammad

A Thesis Submitted in Partial Fulfillment of Requirements  
for the Degree Master of Medical Imaging Technology/  
Functional Imaging Track/ Faculty of Health Professions/  
Al-Quds University

Jerusalem- Palestine

1444/202

Al-Quds University  
Deanship of Graduate Studies  
Faculty of Health profession  
Medical Imaging Technology



## Thesis Approval

# Influence of Iterative Reconstruction Algorithm on Image Quality of Ultra Low-Dose CT Protocol of the Lumbar Spine

Prepared by: Israa Jamal Odeh

Registration Number: 21911023

Supervisor: Dr. Mohammad Hjoui

Master Thesis submitted and accepted, Date: 11.12.2022

The name and signatures of the examining committee members are as follows:

1- Head of the committee: Dr. Mohammad Hjoui

Signature:

2- Internal Examiner: Dr. Hussien ALMasri

Signature:

3- External Examiner: Dr. Montaser Al-Saied Ahmad

Signature:

Jerusalem-Palestine

1444 / 2022

# **Dedication**

This Research is Dedicated to

My Dear Parents, Family, Instructors, and Colleagues

**Declaration:**

I certify that this thesis submitted for the degree of master, is the result of my own research, except where otherwise acknowledged, and that thesis has not been submitted for a higher degree to any other university or institution.

Signed: *israa odeh*

Israa Jamal Odeh

Date: 11/ 12 /2022

## **ACKNOWLEDGEMENT**

May Allah grant us all the blessings of his everlasting life. I would like to extend a special thanks to Dr. Mohammad Hjoui for sponsoring my studies, as well as to collages at the ALLMED center for their support.

Israa J. Odeh

## **Abstract**

Quantitative computed tomography (QCT) or QCT Densitometry is a new examination in computed tomography (CT) used to diagnose bone mineral density. QCT scan is a low-dose protocol with an effective dose value of 1 millisievert (mSv). The dose reduction technique leads to a significant reduction in effective dose at the expense of image quality as it uses the traditional filtered back projection (FBP) method. This study aims to evaluate the impact of the iterative reconstruction (IR) algorithm on image quality and measure the effective dose from low-dose QCT protocol of the lumbar spine CT. This study consisted of 33 patients (all patients files in the selected period) from both genders aged who were clinically suspected of lower back pain and Osteoporosis during the period from 7th July 2021 to the date of ethical approval. Different types of algorithms, FBP, Sinogram Affirmed Iterative Reconstruction (SAFIRE), and iterative beam hardening correction (iBHC) were applied. The image quality criteria including CT number, noise, and signal were analyzed by three regions of interest (ROIs). The three ROIs represent the following anatomy (intervertebral disc, right psoas muscle, and dural sac) respectively, from region 1 – region 3. In addition, for qualitative analysis, the images reconstructed by SAFIRE level 5 (s5) were compared with the grading system by European standards for CT for the evaluation of disc herniation and lumbar spine. The noticed results for the signal-to-noise ratio (SNR) and contrast-to-noise ratio (CNR), showed optimization for images when reconstructed by SAFIRE level 5, with mean SNR of 2.9 which is significantly higher than other reconstruction algorithms ( $p < 0.05$ ). Also, the mean CNR was 2.9 which is significantly higher than other reconstruction techniques ( $p < 0.05$ ). The mean effective dose for the whole population was 1.9 mSv. The SAFIRE algorithm was able to reduce the noise levels at all RIO. The quality of the images according to the grading system by European standards for CT for the evaluation of disc herniation and lumbar spine was similar among the radiologists with good agreement. There is no relationship between body mass index (BMI) and SNR, CNR, and effective dose. In conclusion the use of QCT and using SAFIRE level 5 resulted in higher SNR, CNR, and fewer noise values compared to classic FBP and other levels of SAFIRE. Also, QCT using SAFIRE level 5 revealed equivalent image quality compared to standard protocols of the lumbar spine CT.

## Table of Contents

	<b>Page</b>
Declaration	i
ACKNOWLEDGEMENT	ii
Abstract	iii
Table of Contents	iv
List of Tables	vi
List of Figures	vii
List of Equations	ix
Abbreviations:	x
Chapter 1	1
Introduction	1
1.1 Background of the Study	1
1.2 Problem Statement	5
1.3 Justification	5
1.4 Study Objectives	5
1.5 Study Hypothesis	6
Chapter 2	7
Literature Review	7
2.1 iterative reconstruction Algorithms	7
2.2 Previous Studies	8
2.2.1 Adaptive statistical iterative reconstruction	9
2.2.2 Model based iterative reconstruction	9
2.2.3 Adaptive iterative dose reduction	10
2.2.4 Sinogram Affirmed Iterative Reconstruction	10
2.2.5 iDose <sup>4</sup>	10
Chapter 3	11



Materials and Methods	11
3.1 Study Population and Design	11
3.2 Study Design, Image Acquisitions, and Reconstructions.	11
3.2 Radiation Dose	12
3.3 Data Analysis	13
3.3.1 Quantitative Analysis	13
3.3.2 Qualitative Analysis	14
3.3.3 Statistical Analysis	15
Chapter 4	16
Results and discussion	16
4.1 Study Population	16
4.2 CT Numbers	16
4.3 Noise Values	19
4.4 SNR Values	22
4.5 CNRs Values	23
4.6 SNR as a Function of Patient BMI	24
4.7 CNR as a Function of Patient BMI	25
4.9 Qualitative Analysis	27
Chapter 5	34
5.1 Conclusion	34
5.2 Limitations	34
References	35
Ethical Approval	40
الملخص	41

## List of Tables

	<b>Page</b>
Table 1 Scanning parameters for low-dose lumbar spine CT.....	12
Table 2 Image reconstruction algorithms explanation.....	11

## List of Figures

	<b>Page</b>
Figure 1 For signal-to-noise ratio analysis, various regions of interest are represented. region 1 (intervertebral disc), region 2 (right psoas muscle), and region 3 (dural sac). (Yang et al., 2014). .....	13
Figure 2 The CT number (#) distribution for intervertebral disk (IVD) images reconstructed by 6 algorithms, data distribution for images reconstructed with iterative beam hardening correction (iBHC) exhibit overlaped curves and the images reconstructed without iBHC also exhibit overlaped curves. ....	17
Figure 3 The CT number (#) distribution for psoas muscle images reconstructed by 6 algorithms, data distribution for images reconstructed with iterative beam hardening correction (iBHC) exhibit overlaped curves and the images reconstructed without iBHC also exhibit overlaped curves. ....	18
Figure 4 The CT number (#) distribution for Dural sac (DS) images reconstructed by 6 algorithms, data distribution for images reconstructed with iterative beam hardening correction (iBHC) exhibit overlaped curves and the images reconstructed without iBHC also exhibit overlaped curves. ....	19
Figure 5 The distribution of noise values for the intervertebral disc (IVD) images which were reconstructed using 6 types of reconstruction algorithms, the lowest noise median was using SAFIRE level 5, while the use of filtered back projection (FBP) and iterative beam hardening correction (iBHC) increase noise. ....	20
Figure 6 The distribution of noise values for the Psoas muscle images which were reconstructed using 6 types of reconstruction algorithms, the lowest noise median was using SAFIRE level 5, while the use of filtered back projection (FBP) and iterative beam hardening correction (iBHC) increase noise. ....	21
Figure 7 The distribution of noise values for the Dural Sac (DS) images which were reconstructed using 6 types of reconstruction algorithms, the lowest noise median was using SAFIRE level 5, while the use of filtered back projection (FBP) and iterative beam hardening correction (iBHC) increase noise. ....	22
Figure 8 The influence of 6 types of reconstruction algorithms on SNR of the Dural sac region the highest signal-to-noise ratio (SNR) obtained by SAFIRE level 5, while the lowest median for SNR obtained by SAFIRE level 3 combined with iterative beam hardening correction (iBHC).....	23

Figure 9 The influence of 6 types of reconstruction algorithms on CNR of the Dural sac region the highest contrast to noise ratio (CNR) obtained by SAFIRE level 5, while the lowest CNR obtained by filtered back projection (FBP) combined with iterative beam hardening correction (iBHC).....24

Figure 10 The influence of SAFIRE level 5 reconstruction algorithms on SNR as a function of BMI. ....25

Figure 11 The influence of SAFIRE level 5 reconstruction algorithms on CNR as a function of BMI. ....26

Figure 12 The relationship between radiation effective dose and patient BMI. ....27

## List of Equations

	<b>Page</b>
Equation 1	11
Equation 2	12
Equation 3	13

## **Abbreviations:**

# : Number

3D :Three-dimensional

4D :Four-dimensional

AIDR: Adaptive iterative dose reduction

ASIR :Adaptive statistical iterative reconstruction

BMI :Body mass index

cm :Centimeter

CNR :Contrast-to-noise ratio

CT :Computed tomography

CTDIvol :Computed tomography dose index volume

CTLS :CT scans of the lumbar spine

DLP :Dose-length product

DS :Dural sac

ED :Effective Dose

FBP :Filtered back-projection

HU :Hounsfield units

iBHC :Iterative beam hardening correction

IR :Iterative Reconstruction

IVD :Intervertebral disc

IVF :Intervertebral foramen

k :Conversion factor

Kg :Kilogram

kVp :Kilovoltage peak

L :Level

LD :Low Dose

LDCT :Low-dose CT

m :Meter

mAs :Milliampere-seconds

MBIR :Model-based iterative reconstruction

MD :Mean density

MDCT :Multi-detector CT

mGy :Milligrays

mm :Millimeter

MRI :Magnetic resonance imaging

mSv :Millisievert

PACS :Picture archiving and communication system

PM :Psoas muscle

QCT: Quantitive computed tomography

ROIs :Regions of interest

SD :Standard deviation

SNR :Signal-to-noise ratio

# Chapter 1

## Introduction

### 1.1 Background of the Study

The number of people presenting with spinal-related problems has increased significantly over the past few decades. The main factors that are contributing to this increase are the development of degenerative diseases and the increasing number of people with variable etiologic factors (Dieleman et al., 2016). More effective imaging techniques have been used to diagnose and treat various health conditions, such as spinal disorders (Dieleman et al., 2016). These have led to a rise in total health expenditure (Oxland, 2016). Due to the technological advancements that have occurred in the field of imaging over the past few years, the need for more qualitative indices has increased. This has also resulted in the need for more effective judicial procedures to help improve the efficiency of diagnostic tools (Chou et al., 2011).

The use of IR techniques is commonly used to improve the image quality of CT scans. Compared to traditional methods, it does so by compensating for the higher image noise and the poor image quality (Warncke et al., 2020). In addition, the use of these techniques in clinical practice has led to the reduction of the radiation dosage by up to 65% in the diagnosis of patients and allowed them to provide clinically acceptable images (Hara et al., 2009). In a study, the researchers found that radiation level was significantly reduced after the application of adaptive statistical iterative reconstruction (ASIR) in the lumbar spine CT exam (Alshamari et al., 2017).

A lumbar disc herniation is a type of condition that occurs when the spinal nerve roots and the pulposus tissue of the lumbar intervertebral disc are damaged. It can be caused by various factors such as injury, degeneration, and strain. The tissue of the dura mater, which is located in the outer portion of the spinal canal, can also be pinched or strained. This condition can lead to low back pain and other symptoms such as poor urination (Park et al., 2017). Patients with this condition usually experience low back pain in the early stages. They then develop radiating pain and leg pain in the later stages. In severe cases, it can lead to a disability and a great economic burden (Booz et al., 2019).



Intervertebral disc herniation is caused by the rupture of the fibers, which can be due to various reasons such as chronic strain and lumbar degeneration. The nucleus pulposus then moves laterally or backward. (Zheng et al., 2021) . The effects of the spinal nerve root stimulation and the cauda equina on the lower back are usually accompanied by pain and numbness in the limbs. This condition is very serious, affects the lives, and work of patients. It can be caused by various factors such as the long-term presence of the disease and its complications. Modern medicine has helped people gain a deeper understanding of the disease. Due to the increasing prevalence of lower back and leg pain, it has become one of the main threats to human health. The aging population and the increasing severity of the condition have caused a huge burden on society. Some of the factors that can trigger low back pain are the degeneration of the lumbar facet joints and the compression of the nerve roots (Zheng et al., 2021).

Complex anatomical and soft tissue components, as well as the varying osseous elements and projections, make spinal imaging challenging. The early days of radiography were focused on assessing the spinal structures (Oxland, 2016). Early in the field of radiology, plain radiography was used to assess the spinal structure(Hoeffner et al., 2012). X-ray imaging for the diagnosis of spinal disorders has been regarded as the primary technique used in this field. It can be used to examine the alignment of the vertebral body and the size of the bone space. Although radiography can be used to diagnose a variety of spinal disorders, it is not the gold standard for the diagnosis of these conditions(Tang & Aggarwal, 2013). For instance, it cannot provide detailed information about the nerve roots and spinal cord. This technique is commonly used to visualize the spinal cord, paravertebral soft tissues (including the spinal cord and the vertebral column), and bone marrow involvement. However, its performance in these areas is not satisfactory. In addition, it is not ideal for evaluating small anatomic structures, such as intervertebral foramen (IVF) and facet joints (Yang et al., 2014).

CT provides a more accurate and precise demonstration of the various components of the intervertebral disc (IVD), including the facet joints, foramina, and fractures (Yang et al., 2014). It also allows for more precise planning during the surgical procedure (Warncke et al., 2020). It is commonly used for the diagnosis of morphologic changes and is a recognized tool for the diagnosis of a herniated disc (Lurie, 2005). The advantages of CT over magnetic resonance imaging (MRI) are its lower cost, shorter testing time, and

availability in hospitals. However, it comes with some drawbacks, such as exposure to ionizing radiation.

The number of CT examinations has increased significantly around the world, which has led to an increase in the radiation dose (Arjah, Hamza, Hjouj, 2020). It has been theorized that this increase in exposure could lead to an increased risk of developing cancer. Due to the seriousness of the issue, awareness campaigns have been launched to raise awareness of both the hazards of medical radiation and the need to reduce them. CT scans of the lumbar spine can also expose various sensitive organs, such as the gastrointestinal tract, bone marrow, and genital organs. Although the actual dose for lumbar CT of radiation that can be given to these organs is around 4.1 millisieverts (S. H. Lee et al., 2018), it has been reported that the dose can go up to (19 mSv) (Warncke et al., 2020).

To minimize the amount of radiation that's produced by standard CT scans, the as low as reasonably achievable (ALARA) principles should be followed. This can be done through the reduction of the dose of ionizing radiation without compromising the quality of the images (Yang et al., 2014). Conventional radiography is often used to minimize radiation exposure. To avoid using "standard" CT, clinicians may utilize this modality at a lower dose. Doing so can lead to reduced image quality and increased noise, though it can still be performed at a relatively low dose. Compared to radiography, CT at this level may provide a higher level of diagnostic value and detail regarding anatomical changes (McCullough et al., 2012), (Thrall J., 2012), (Alshamari et al., 2014), (Arjah et al., 2019).

Although conventional radiography is commonly used to minimize radiation exposure, some clinicians may opt for a lower-dose CT scan instead of "standard" CT to avoid experiencing issues such as poor image quality and noise (Yang et al., 2014). This type of imaging can still provide a more accurate and detailed analysis of anatomical changes. Although the standard-dose CT protocols can be used for low-dose CT (LDCT) examinations with an effective dose for lumbar CT around 2.6 mSv (S. H. Lee et al., 2018), (Weinrich et al., 2018), they are not ideal for the diagnosis of the lumbar spine region. In order to achieve the best possible image quality, settings need to be adjusted. LDCT. LCT is a recent technique that is commonly used to examine the spinal region using a low dose of radiation around 1 mSv. Compared with standard-dose CT, this

procedure has reduced image quality and increased image noise(Alshamari et al., 2017). Due to the improved image quality and reduced dose, iterative reconstruction is commonly used in CT. This technique was recently integrated into the ultra-low-dose and low-dose protocols instead of the classic filtered back-projection (FBP) (S. H. Lee et al., 2018).

For decades, CT image reconstruction has been done using FBP. This technique assumes that the geometry of the images can be adjusted to reduce the noise and improve the reconstruction speed (Hamza et al., 2022) (Omarah et al., 2022). However, this method also adds to the image noise (Wurdeman et al., 2017),(Singh et al., 2010). Due to the increasing complexity of the process and the cost of processing, CT vendors started developing new methods ten years ago. The goal of IR is to reduce the radiation dose and image noise(Singh et al., 2010), (Toshiba, 2012), (Andersen et al., 2018),(Grant & Raupach, 2012),(D. Mehta et al., 2013), (Godt et al., 2021),(Willemink et al., 2013a). One of the techniques that are commonly used in hybrid reconstruction, is faster than traditional iterative techniques. This method aims to achieve a better quality of CT images while preserving the details (Singh et al., 2010), (Toshiba, 2012), (Grant & Raupach, 2012), (D. Mehta et al., 2013). Hybrid techniques are used in both image space and projection space, and they can be used with both iterative and blended techniques of FBP (Omarah et al., 2022). Some vendors also offer model-based techniques, which combine the effects of photon and noise statistics with scanner geometry and optics. These techniques can reduce artifacts and noise, but they can also alter the image texture due to denoising that can modify anatomical edge (Willemink et al., 2013b).

Both image quality and the diagnostic value are affected by various factors such as the choice of imaging parameters, the post-processing algorithm, and the mode of display. Through IR techniques, which are based on a correction loop, a further dose reduction can be achieved, resulting in a dose exposure level that's comparable to that of standard radiographs. Unlike traditional FBP techniques, IR methods do not alter CT attenuation values because is is correct the sinogram projection and remove the noise in image space. They can also reduce image noise without affecting the signal-to-noise ratio (SNR) and contrast-to-noise ratio (CNR) which lead to improving the overall image quality and diagnostic image. According (Omoumi et al., 2014), in multi-detector CT(MDCT), the dose reductions in the lumbar spine CT have been reported to be 50% from the full dose. In

contrast to conventional back-projection reconstruction, the image noise can be reduced by 31% and the radiation dose by 52% by utilizing the IR algorithm (S. H. Lee et al., 2018).

## **1.2 Problem Statement**

The increasing number of patients who undergo CT scans of the lumbar spine (CTLS) for various conditions has raised concerns about their safety. CTLS scans expose patients to high levels of radiation which can reach up to 19 mSv (Warncke et al., 2020). In addition to the lifetime risk of getting radiation-induced cancer, this concern is also about hereditary defects. This is especially true for younger individuals (Yang et al., 2014). Low dose protocol reconstructed by FBP cannot remove the image noise for both signal-to-noise ratio (SNR) and contrast-to-noise ratio (CNR) will be decreased which leads to reduce the overall image quality and diagnostic value of the images. In order to improve the overall image quality, image noise and the dose that is used in CTLS can be reduced (Yang et al., 2014). Also, to minimize radiation exposure, clinicians may use a low-dose lumbar spine technique in combination with IR to avoid using "standard" CT.

## **1.3 Justification**

The increasing performance of CT examinations has led to the need for reduced-dose scanning in clinical practice. This procedure can be performed safely and effectively by optimizing the radiation dose. However, it is also important to note that the quality of the images is also important to diagnose and visualize diseases (S. H. Lee et al., 2018). The goal of low-dose CT with IR is to minimize the radiation dose and image noise that can be generated by the FBP technique. This method can be performed with a minimal dose of radiation. Currently, the only method of performing this procedure is with a low-dose protocol with an effective dose of 1.0 to 3.4 mSv (S. H. Lee et al., 2018).

## **1.4 Study Objectives**

This study has multiple goals:

1. To evaluate the impact of the iterative reconstruction (IR) algorithm on image quality by using objective and subjective metrics for low-dose quantitative computed tomography (QCT) protocol of the lumbar spine CT.

2. To measure the effective dose from low-dose lumbar spine protocol using data acquired from patient dose report.

### **1.5 Study Hypothesis**

We hypothesized that low-dose CT with IR performed similarly to standard-dose CT in terms of its diagnostic performance when used with a lower effective dose. In this study, the researchers examined the various factors that affect the image quality and accuracy of this technique.

## Chapter 2

### Literature Review

#### 2.1 iterative reconstruction Algorithms

Some CT manufacturers have started implementing various iterative reconstruction techniques to reduce image noise and improve spatial resolution. (T. Y. Lee & Chhem, 2010),(Fleischmann & Boas, 2011),(Willemink et al., 2013a),(Winklehner et al., 2011). All of the manufacturers have their IR methods. For instance, General Electric had developed adaptive statistical iterative reconstruction (ASIR), and model-based iterative reconstruction (MBIR). Similarly, the adaptive iterative dose reduction (AIDR) for Toshiba and the Sinogram Affirmed Iterative Reconstruction (SAFIRE) for Siemens, and (iDose) which is the fourth-generation hybrid iterative reconstruction algorithm introduced by Philips.(Willemink et al., 2013),(Miéville et al., 2013). ASIR is a hybrid iterative reconstruction (IR) algorithm introduced by GE that uses a blend of filtered back-projection (FBP) with iterative reconstruction images in the raw data domain to reduce image noise (Omarah Naser Saed Abd Alqader, 2021). ASIR performs a hybrid iterative process of mathematical and statistical modeling to identify and selectively reduce the noise of an image(Willemink et al., 2013).AIDR is a hybrid reconstruction algorithm, introduced by Toshiba, which statistical model in combination with an imaging model that is used on the raw data to reduce noise and artifacts. The iterations are executed in image space only, where edge preservation and smoothing are performed. The corrected image is blended with the initial image (from the raw data) to keep the noise granularity. There are three different levels of iteration with different iterative strengths: mild, standard, and strong(Miéville et al., 2013). Like SAFIRE, these algorithms are usually performed in the raw data or the image domain. SAFIRE is a unique CT iterative reconstruction algorithm that uniquely allows for up to 60% lower radiation dose in CT examinations without compromising image quality. The strength levels are set by the manufacturer(Willemink et al., 2013),(Winklehner et al., 2011). The strength level of IR can be affected by the number of iterations and the proportion of FBP and IR in the final multi detector CT (MDCT) images. With SAFIRE, the noise models' approximations and estimations are set up differently for each strength level. For instance, the stronger the model's goal is,

the more noise it can reduce (Willemink et al., 2013),(Miéville et al., 2013).

In a previous study, ADIR was shown to improve the image quality and reduce the radiation dose compared to standard FBP. The results of the study indicated that IR could potentially decrease the radiation dose (Gervaise et al., 2012). In another study, the level of radiation that was delivered to the lumbar spine after using IR decreased. The computed tomography dose index volume (CTDI<sub>vol</sub>) for lumbar spine CT (LSCT) showed that the dose levels were  $22.6 \pm 8.2$  for images reconstructed using the FFB technique and  $18.0 \pm 6.3$  for those using IR (Komlosi et al., 2014).

A study on patients with full-dose lumbar spine CT and low-dose CT examinations using the tube voltage 120 and 100 kV settings. They compared the image quality and radiation levels with those of the control group. At about 50% lower dose, the low-dose reconstructions using IR provided equivalent diagnostic reliability and image quality compared to standard CT procedures. The results indicated that low-dose CT reconstructions using IR provided comparable diagnostic reliability and image quality to those using standard full-dose CT procedures.(Alshamari et al., 2017).

## **2.2 Previous Studies**

In other regions, low-dose CT is commonly used for assessing the diagnostic accuracy of urolithiasis. According to a review conducted by (Niemann et al., 2008), the overall accuracy of this test was 99.32%. Lung cancer screening using low-dose CT can reduce mortality by 20% (S. R. et al Mehta, 2015). This modality can be used for patients with a regular heart rate and a history of coronary stenoses (Scheffel et al., 2008). It can also detect polyps and colorectal cancers (Alshamari et al., 2016).

Two studies have shown that low-dose (CT) is more accurate than plain radiographs when treating the lumbar spine. The other study shows that it is feasible to perform this procedure at an effective dose of around 2.6 to 0.9 mSv in humans(S. H. Lee et al., 2018),(Weinrich et al., 2018). According to European and American national diagnostics, the CTDI<sub>vol</sub> reference levels for the lumbar spine are as high as 16 mGy. Also, revealed that the reference levels for CTDI<sub>vol</sub> for the lumbar spine, CT is reported to be up to 19 mGy (Warncke et al., 2020).

A previous study also indicated that increasing the strength of SAFIRE by 10% can reduce image noise by about 10% (Omoumi et al., 2014). In addition, Gervaise and colleagues noted that using IR techniques in the MDCT can reduce radiation doses by up to 50% (Weinrich et al., 2018). There have been various protocols for lumbar spine CT using low-dose (LD) radiation. This modality is commonly used as a replacement for standard-dose radiography for the diagnosis of lumbar spine conditions with an effective dose range from 1-4 mSv (S. H. Lee et al., 2018).

The studies concluded that the use of LDCT could be beneficial for diagnosis before treating lower back pain. They found that the images produced by this technology were better than those of lumbar radiography (Alshamari et al., 2016). LDCT scans of the lumbar spine revealed a significant improvement in image quality compared to standard CT scans. The images were also more accurate and produced better reproductions of various anatomical structures. Some of these include the trabecular bone, cortical bone, intervertebral joints, and disk profile (Alshamari et al., 2017).

Studies have shown that an increase in the IR level can reduce noise. Others claim that the noise spectrum shifts to the lower frequencies. This suggests that the images may have an over-smooth appearance due to the shift in the noise spectrum (Alshamari et al., 2017).

### **2.2.1 Adaptive statistical iterative reconstruction**

The technique, called adaptive statistical iterative reconstruction (ASIR) by its developer, GE Healthcare, reduces noise in the image, allowing a downward adjustment in radiation dose to obtain standard diagnostic quality images. Patient radiation doses were reduced up to 65% using the low-dose IR method (GE Healthcare, n.d.).

### **2.2.2 Model based iterative reconstruction**

statistical model based iterative reconstruction (MBIR) method has been introduced for clinical use. Based on the principle of MBIR and its nonlinear nature, the noise performance of MBIR is expected to be different from that of the well-understood filtered backprojection (FBP) reconstruction method (Li et al., 2014).



### **2.2.3 Adaptive iterative dose reduction**

adaptive iterative dose reduction (AIDR) (Toshiba Medical Systems) is an iterative algorithm for performing noise reduction techniques in the raw data and image domain. Processing in the raw data domain involves a statistical model, scanner model, and projection noise estimation to decrease noise. Then in the image domain an iterative noise reduction technique is applied to optimize the reconstruction (Joemai et al., 2013).

### **2.2.4 Sinogram Affirmed Iterative Reconstruction**

Involves 2 different iterative correction loops Corrections first performed on the raw data to remove image artifacts, before noise reduction in the image space, the use of SAFIRE at lower doses generally resulted in superior or similar image quality to full-dose FBP images amount of improvement in image quality with the use of SAFIRE is lesser in patients of heavier weights (>75kg) or obese patients (Qiu & Seeram, 2016).

### **2.2.5 iDose<sup>4</sup>**

Fourth-generation hybrid iterative reconstruction algorithm introduced by Philips, this CT scan parameter can be turned off or on. This new technique provides a genius solution for SNR improvement in which iterative processing is performed in both the image domains and projection. The first filtering performed for projection data, where it performs correction for the noisiest CT measurements. Through an iterative diffusion process, the noisy data is canceled without edge disturbances. The second filtering of the iDose4 deals with a subtraction of the CT image noise while saving the edges associated with anatomy (Arjah, Hamza, Hjouj, 2020).

## Chapter 3

### Materials and Methods

#### 3.1 Study Population and Design

This study was retrospectively conducted on all patients from both genders aged 18 to 76 years who were clinically suspected of lower back pain and osteoporosis during the period from 9<sup>th</sup> October 2022 to the date of ethical approval. Furthermore, the patients who underwent follow-up assessments were also included in the study. The study population during this period who had been diagnosed with Osteoporosis or lower back pain was a sum of 33 patients. The study was approved by the Ethics Committee of Al-Quds University. The study was conducted to ensure that the safety of non-invasive procedures was maintained without additional burden to public health. It was conducted in a manner that ensured the full confidentiality of both the patients and their medical records.

#### 3.2 Study Design, Image Acquisitions, and Reconstructions.

Lumbar spine CT examination was performed in a single radiology center using a single multi-detector CT machine: SOMATOM GO. Now CT, 16-row scanner (Siemens Healthcare). Low-Dose QCT protocol was applied. Helical scans from the lower thoracic spine to the sacrum were performed with a field of vision of 32 to 36 cm, a matrix size of 512\*512, and both standard body regular (Br36) soft kernel and sharp (Br56) kernels were used for soft tissue and bone respectively. Automatic tube current modulations (CARE-DOSE 4D) were used on during the scan for all patients. CARE Dose 4D system automatically adjusts the tube current based on the X-ray attenuation changes and the patient's size. This feature is performed during each rotation of the tube to maintain the ideal current. The user-defined reference product for tube current measurement is used to set the stage for the adaptation (Söderberg, 2016). Table 1 shows the scanning parameters for the low-dose protocol. The reformations of sagittal, axial, and coronal multiplanar reconstruction (MPR) were sent to the picture archiving and communication system (PACS). To minimize the radiation dose and maintain the quality of the images, SAFIRE level 3 is used in all examinations. This method uses a noise modeling technique to estimate the noise content in the raw data set. It then removes it from the image data

after each iteration. (Shin et al., 2013). Furthermore, to remove the beam hardening artifacts from images, the proposed method, known as iterative beam hardening correction (iBHC), was used to reconstruct the computed object's linear attenuation coefficients using the obtained polychromatic projections (Zhao & Li, 2015). Table 2 shows the image reconstruction algorithms explanation.

Table 1: Scanning parameters for low-dose lumbar spine CT.

Scan Parameters	Setting
Collimation	16 * 7 mm
Slice thickness	2 mm
Pitch	0.8
Rotation time	1 s
kVp	80
Effective mAs	128
Dose modulation	CARE-DOSE 4D

Table 2 Image reconstruction algorithms explanation

Recon name	Reconstruction Explanation
<b>FBP</b>	The image reconstructed by conventional technique filtered back projection (FBP)
<b>S3</b>	The image was reconstructed using SAFIRE level 3
<b>S5</b>	The image was reconstructed using SAFIRE level 5
<b>FBPi</b>	The image reconstructed by conventional technique FBP in combination with iBHC
<b>S3i</b>	The image was reconstructed using SAFIRE level 3 in combination with iBHC
<b>S5i</b>	The image was reconstructed using SAFIRE level 5 in combination with iBHC

### 3.2 Radiation Dose

The CT dose index volume (CTDIvol) and dose-length product (DLP) were generated automatically by the system for each examination has been recorded. The effective dose was calculated by considering the lumbar spine's conversion factor ( $0.011 \text{ mSv}^{-1} \times \text{mGy}^{-1} \times \text{cm}^{-1}$ ) and multiplying the DLP (mGy-centimeter) according to the following equation(Yang et al., 2014):

$$ED = k \times DLP \dots \dots \dots (1)$$

### 3.3 Data Analysis

#### 3.3.1 Quantitative Analysis

Real quantitative measurements were carried out by RadiAnt software version 2022.1.1. Most of the patient's symptoms were caused by abnormalities at the L4–L5, L5–S1 levels, and below the iliac bones. These levels were the focus of our study. At the L4/L5 levels, the mean density (MD) in Hounsfield units (HU) and standard deviation (SD) were measured at four regions of interest (ROIs), including the intervertebral disc (IVD), the Dural sac (DS), the right psoas muscle (PM), and the trabecular bone of the L5 vertebral body (Figure. 1). Region 1 was drawn as large as possible to cover the whole region and avoid significant noise and fat infiltration with a diameter of 20 mm<sup>2</sup>. Region 2 had a diameter of 20 mm<sup>2</sup>, and region 3 had a diameter of 20 mm<sup>2</sup> minimizing partial volume effects in these regions and ensuring that regions are in the middle of the anatomical structure. The signal-to-noise ratio (SNR) of each area was determined by the following equation (Yang et al., 2014):

$$\text{SNR} = \frac{\text{CT number}}{\text{SD}} \dots\dots\dots (2)$$

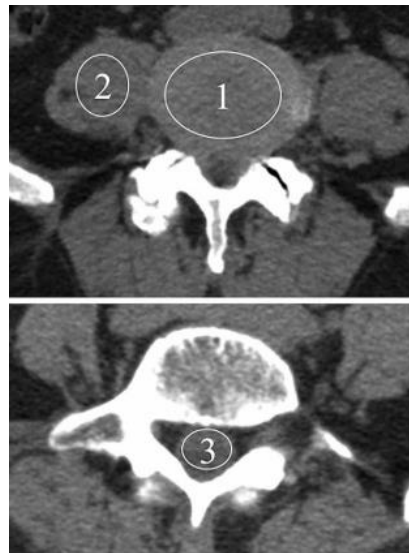


Figure 1 For signal-to-noise ratio analysis, various regions of interest are represented. region 1 (intervertebral disc), region 2 (right psoas muscle), and region 3 (dural sac). (Yang et al., 2014).

The CNR difference in the contrast-to-noise ratio (CNR) between the DS and IVD is a calculation that shows the difference between the two interfaces as the following equation (Yang et al., 2014):

$$\text{CNR} = \frac{(\text{MD IVD} - \text{MD DS})}{(\text{SD}^2\text{IVD} + \text{SD}^2\text{DS})^{\frac{1}{2}}} \dots \dots \dots (3)$$

### 3.3.2 Qualitative Analysis

The two radiologists, who were both board-certified in their field, were unaware of the acquisition parameters of the images. They then independently reviewed the images for SAFIRE s5 that were placed on the PACS system. The information collected from patients was kept anonymous. The readers can customize the setting to their preferences. The grading system was based on European standards for computed tomography for the evaluation of disc herniation and lumbar spine (European Guidelines for DECT, 2004) :

1. Visually sharp reproduction of the intervertebral disk profiles
2. Visually sharp reproduction of the thecal sac
3. Visually sharp reproduction of the perithelial fat
4. Visually sharp reproduction of the intervertebral radicular canals
5. Visually sharp reproduction of the nerve roots
6. Reproduction of the cortical and trabecular bone
7. Visually sharp reproduction of the intervertebral joints
8. Reproduction of the paravertebral ligaments

The reviewers gave each standard a score of 0, convinced that the standard is not fulfilled, with one being somewhat confident that it wasn't fulfilled, two being indecisive about whether or not it was, three being somewhat confident that it was, and four convinced the standard is fulfilled.

### **3.3.3 Statistical Analysis**

The data manipulation for this study was carried out using inferential and descriptive statistical methods. The analysis was performed using Microsoft Excel. The t-test was used to compare the two independent population means. Also, a z-test was performed for two population proportions. The first was for the proportion of the quality criteria that matched the 8 criteria used in the low-dose lumber CT and the second was for the proportion of the criteria that matched the 8 criteria used in the 31 mGy CTDIvol (Calzado et al 2000). A value of  $p < 0.05$  was used as a significance standard (Plichta & Kelvin, 2021).

## Chapter 4

### Results and discussion

#### 4.1 Study Population

The study was conducted on 33 patients who had undergone QCT scans. The study population was composed of 29 females and 4 males. The mean age of the patients was 57.7 years ranging from (19 - 77 years). The mean score of the patient's weight was 79.42 Kg (49 - 110 Kg) with a mean body mass index (BMI) value of 30 kg. /m<sup>2</sup> (22 - 40 kg. /m<sup>2</sup>). More than two-thirds of patients were obese.

#### 4.2 CT Numbers

Figure 2 displays the deviated CT numbers for the intervertebral disc region while using different types of reconstruction algorithms at a 110 kVp setting. The mean values for CT numbers were 84.7, 84.5, and 85.4 for SAFIRE S5, SAFIRE s3, and FBP respectively. Using the SAFIRE algorithm, the CT number values for IVD increased from the baseline algorithm (FBP) and were most noted when SAFIRE s5 was used without any significant changes with FBP (p= 0.08) or SAFIRE s3 (p= 0.09). On the other hand, when iBHC was combined with SAFIRE and FBP, CT number values showed significant changes with a mean value of 95.6, 96. and 96.9 for SAFIRE s5, SAFIRE s3, and FBP respectively. The images reconstructed with FBP integrated with the iBHC algorithm showed a significant increase in CT number values (p<0.001) compared to FBP alone and over both levels of the SAFIRE algorithm without iBHC (p<0.002).

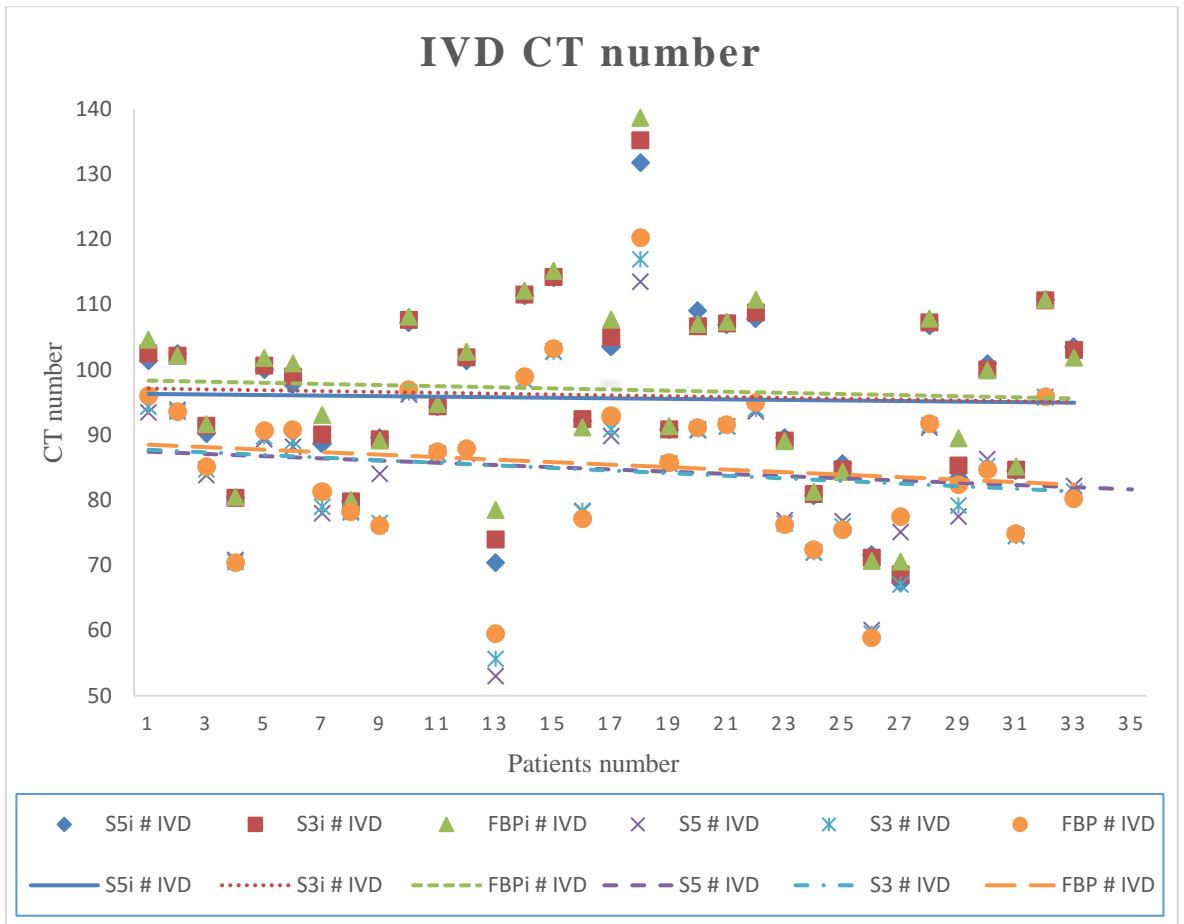


Figure 2 The CT number (#) distribution for intervertebral disk (IVD) images reconstructed by 6 algorithms, data distribution for images reconstructed with iterative beam hardening correction (iBHC) exhibit overlaped trend lines and the images reconstructed without iBHC also exhibit also overlaped trend lines.

As shown in Figure 3, for the right psoas muscle region, the mean values for CT numbers were 54.64, 54.36, and 54.30 for SAFIRE s5, SAFIRE s3, and FPB respectively. Using the SAFIRE algorithm has no impact or any significant changes ( $p > 0.05$ ) on the CT number values for psoas muscle compared to the FBP algorithm. Although when iBHC was combined with SAFIRE and FBP, the mean values of CT number values were increased by 0.8%, and there were significant changes compared to both FBP and SAFIRE algorithms alone ( $p < 0.001$ ).



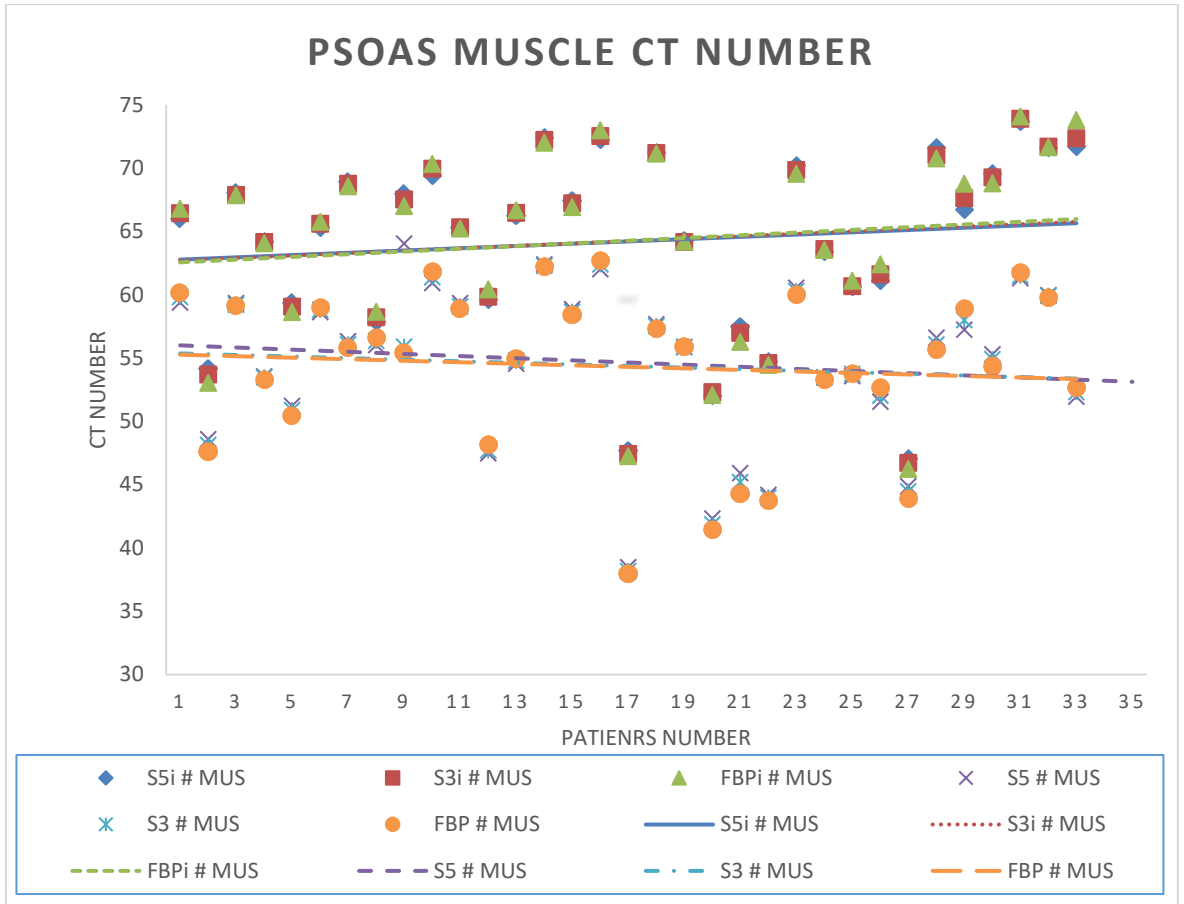


Figure 3 The CT number (#) distribution for psoas muscle images reconstructed by 6 algorithms, data distribution for images reconstructed with iterative beam hardening correction (iBHC) exhibit overlaped trend lines and the images reconstructed without iBHC also exhibit overlaped trend lines.

For the Dural sac region, the mean values for CT numbers were 17, 17.74, and 18.4 for SAFIRE s5, SAFIRE s3, and FPB respectively. Using the SAFIRE algorithm has no impact or any significant changes ( $p>0.05$ ) on the CT number values compared to the FBP algorithm. Also, when iBHC was combined with SAFIRE and FBP, CT number values had no significant changes ( $p>0.05$ ) with a mean value of 22.8, 23.4, and 24.2 for SAFIRE s5, SAFIRE s3, and FPB respectively (Figure 4).

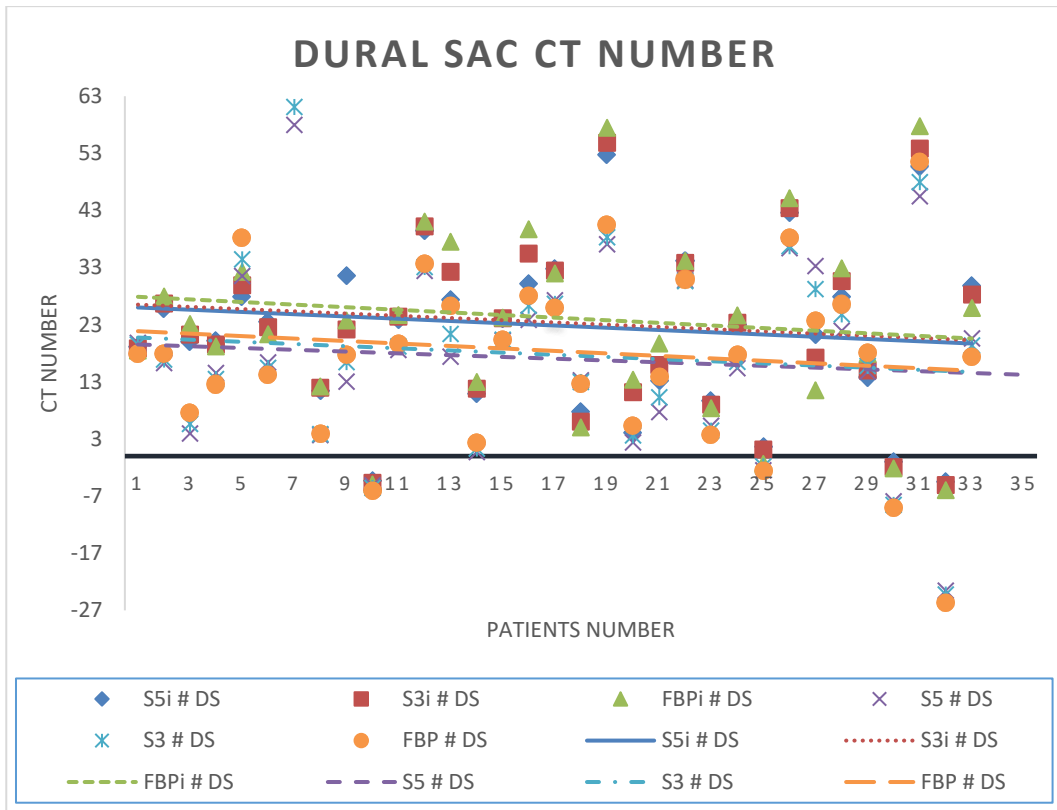


Figure 4 The CT number (#) distribution for Dural sac (DS) images reconstructed by 6 algorithms, data distribution for images reconstructed with iterative beam hardening correction (iBHC) exhibit overlaped trend lines and the images reconstructed without iBHC also exhibit trend lines.

### 4.3 Noise Values

The standard deviation of pixels in the ROIs has been used to quantify the noise of the ROIs. The usage of the SAFIRE algorithm reduces the noise values of the IVD region (Figure 5). The mean noise value for IVD was 22, 26, and 30 for SAFIRE S5, SAFIRE s3, and FPB respectively. Compared to the other methods, the reconstruction of SAFIRE images with SAFIRE s5 yielded the most noise reduction with significant noise reduction than FBP ( $p < 0.05$ ). Although the SAFIRE algorithm reduces the noise values, it showed a negative effect when combined with iBHC and make worse. For instance, when combined with the iBHC algorithm, noise values increased for FBP, SAFIRE s3, and SAFIRE s5 with a mean value of around 85% compared to FBP and SAFIRE alone.

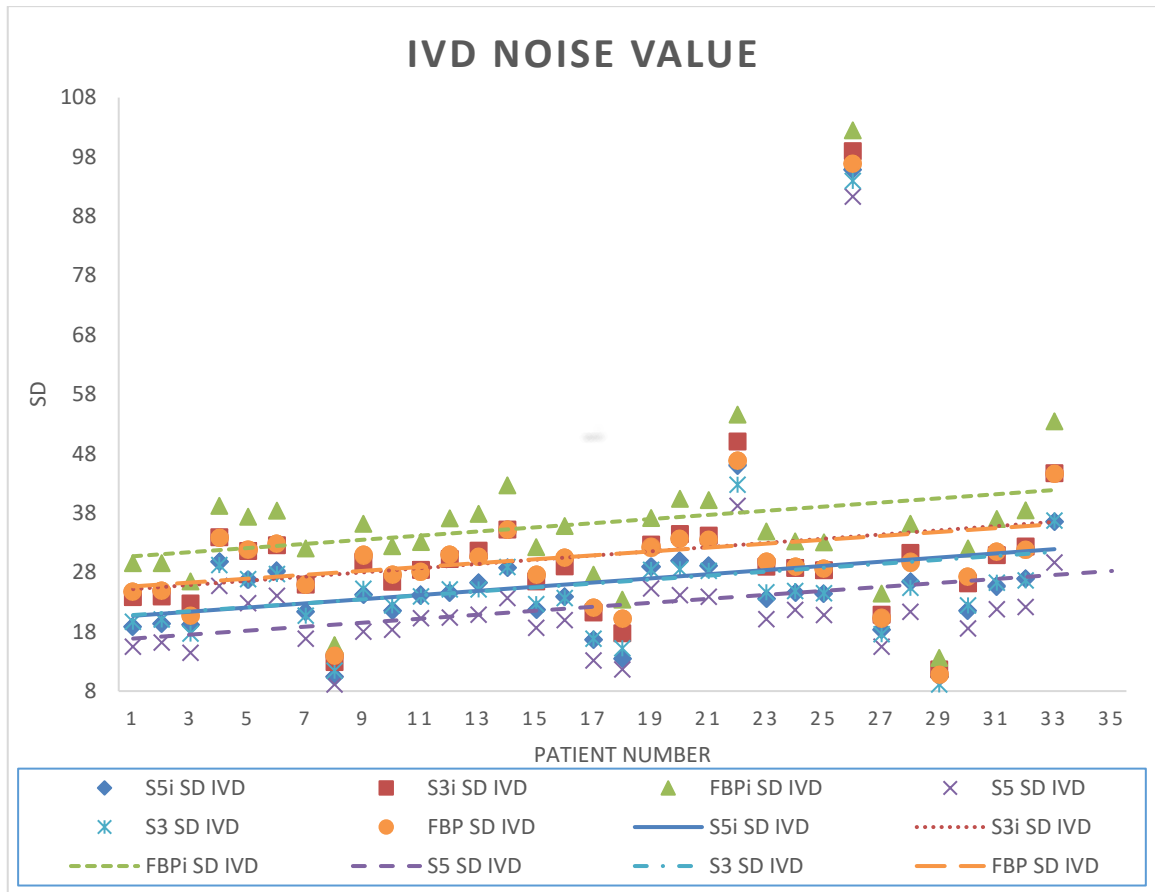


Figure 5 The distribution of noise values for the intervertebral disc (IVD) images which were reconstructed using 6 types of reconstruction algorithms, the lowest trend line was using SAFIRE level 5, while the use of filtered back projection (FBP) and iterative beam hardening correction (iBHC) increase noise and provide higher trend line however the highest trend line obtained by FBPi reconstruction.

The SAFIRE algorithm was able to reduce the noise levels in the right psoas muscle (Figure 6). The mean noise value for the psoas muscle was 19.75, 23.9, and 28.7 for SAFIRE S5, SAFIRE s3, and FPB respectively. SAFIRE s5 shows a significant noise reduction compared with SAFIRE s3 and FPB ( $p < 0.001$ ). On the other hand, noise values were increased when SAFIRE and FBP integrated with iBHC by 0.85%. The mean noise values were significantly increased for FBP ( $p < 0.05$ ), and SAFIRE s5 ( $p < 0.001$ ).

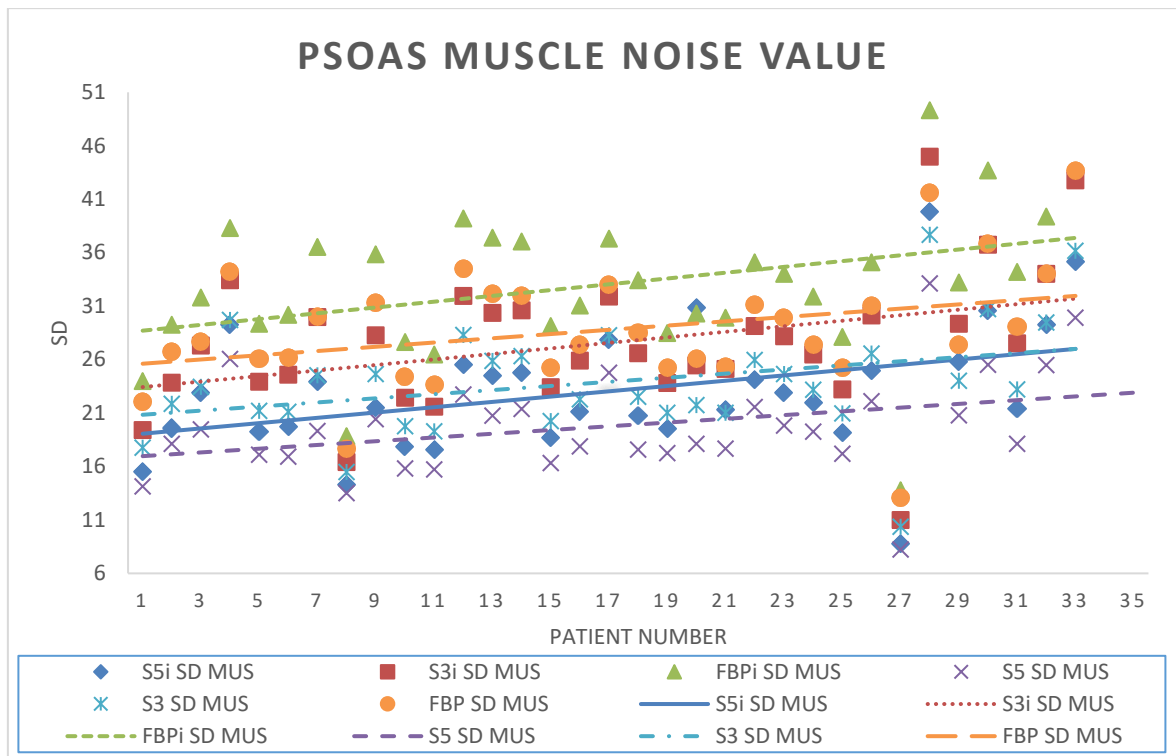


Figure 6 The distribution of noise values for the psoas muscle images which were reconstructed using 6 types of reconstruction algorithms, the lowest trend line was using SAFIRE level 5, while the use of filtered back projection (FBP) and iterative beam hardening correction (iBHC) increase noise and provide higher trend line however the highest trend line obtained by FBPi reconstruction.

The mean noise values for the dural sac were 13.2, 16.4, and 20.6 for SAFIRE S5, SAFIRE s3, and FPB respectively (Figure 7). SAFIRE had a good impact in reducing noise values in the dural sac and was most effective when using SAFIRE level 5. SAFIRE s5 had a significant noise reduction compared to FPB ( $p < 0.001$ ). Although the overall noise was slightly increased when SAFIRE paired with iBHC, with a mean value of noise of 14.7, 18.2, and 23.2 for SAFIRE S5, SAFIRE s3, and FPB respectively, SAFIRE s5 with iBHC leads to significant noise reduction compared to FPB with and without iBHC ( $p < 0.05$ ).

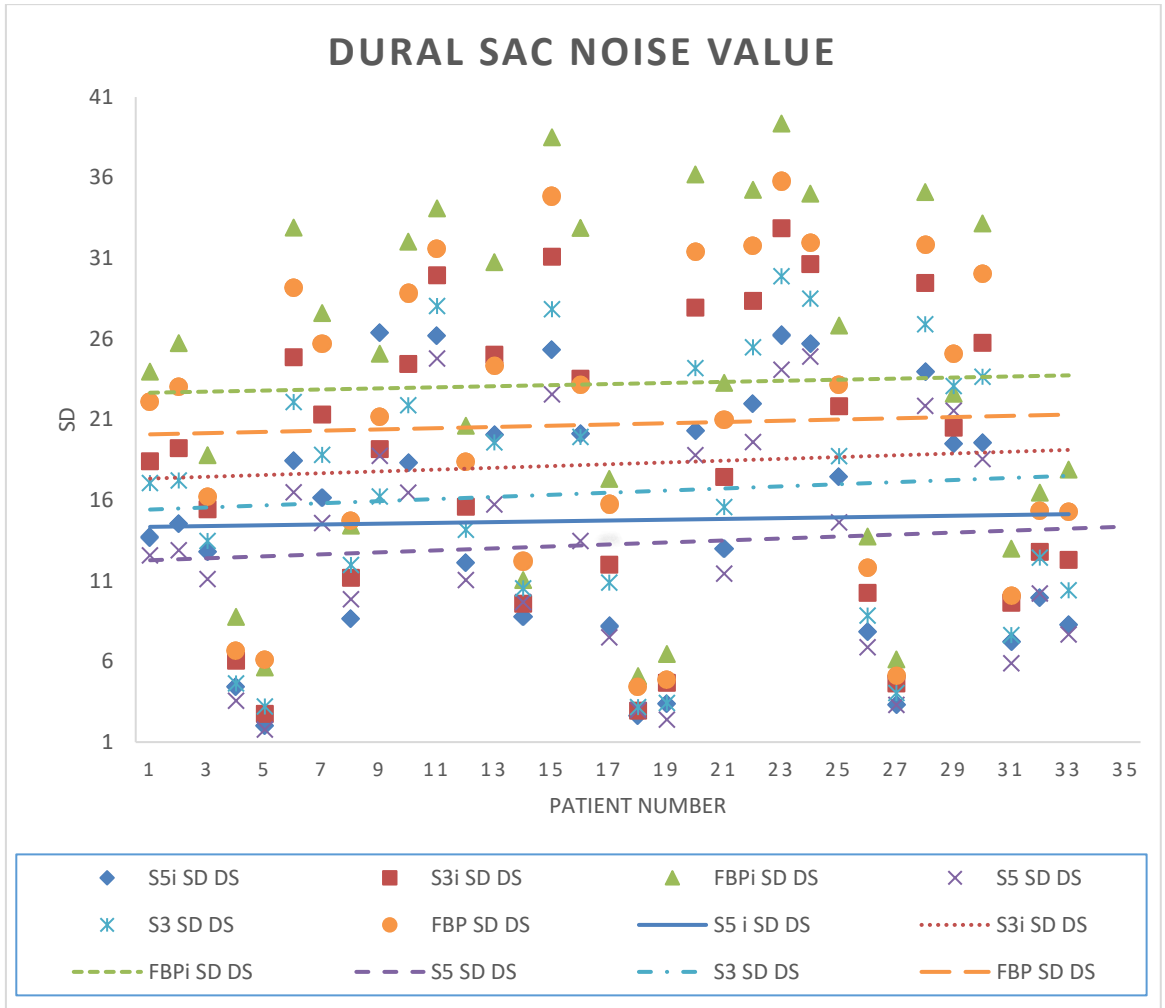


Figure 7 The distribution of noise values for the dural sac (DS) images which were reconstructed using 6 types of reconstruction algorithms, the lowest trend line was using SAFIRE level 5, while the use of filtered back projection (FBP) and iterative beam hardening correction (iBHC) increase noise and provide higher trend line however the highest trend line obtained by FBPi reconstruction.

#### 4.4 SNR Values

The SAFIRE algorithm was able to improve the overall SNR and make the dural sac clear again (Figure 8). The mean SNR improvements were 2.9, and 2.2 for SAFIRE s5 and s3 respectively in comparison with the reference SNR value (1.6) for FBP. Concerning iBHC, the Overall SNR was slightly higher for SAFIRE s5 alone (2.9) than for images that combined SAFIRE s5 and iBHC (2.8). Also, the integration between iBHC and FBP had no impact on FBP images alone. For SAFIRE s3, there was a significant decrease in SNR values of around 40% when combined with iBHC ( $p < 0.05$ ).

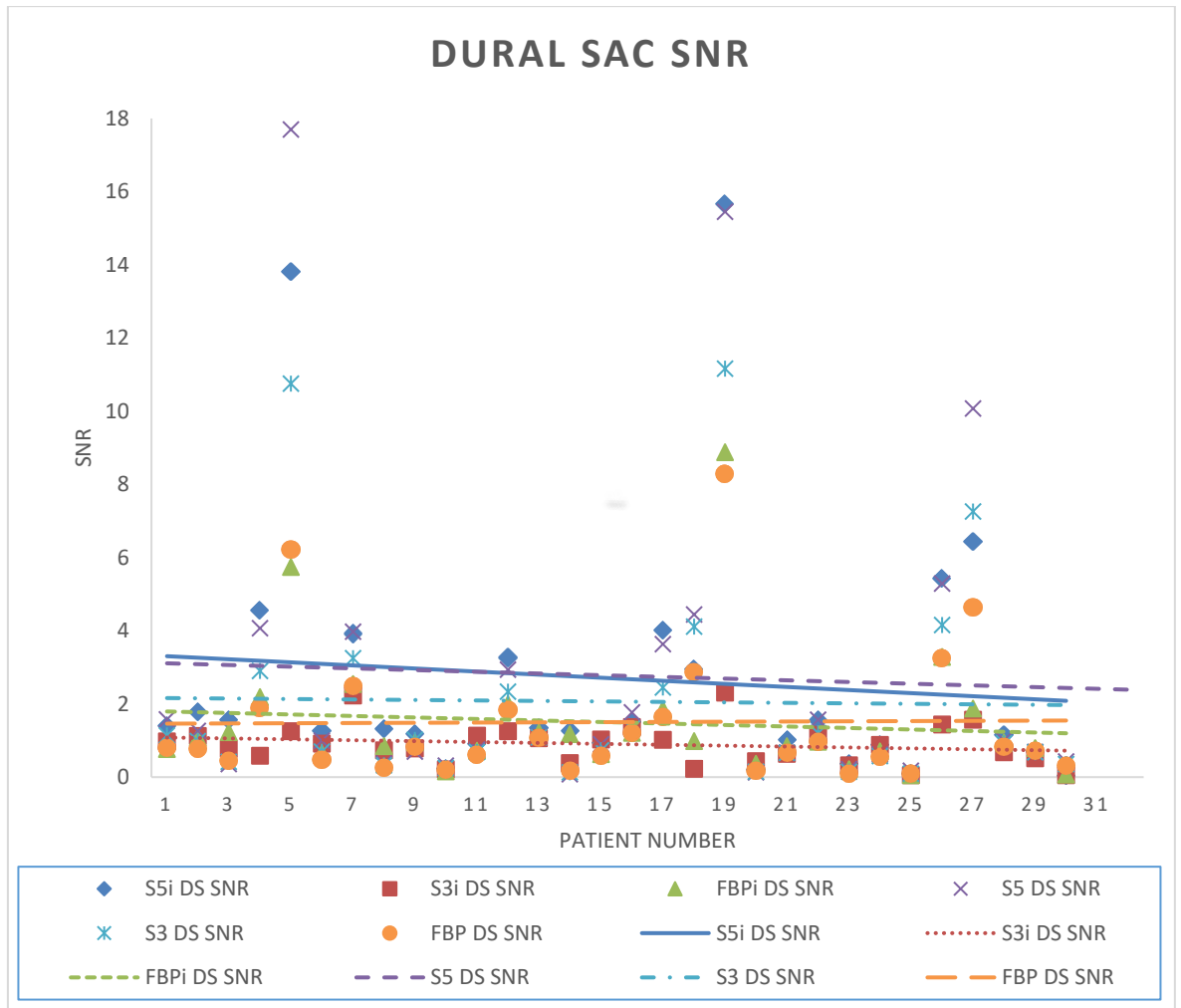


Figure 8 The influence of 6 types of reconstruction algorithms on SNR of the Dural sac region the highest signal-to-noise ratio (SNR) obtained by SAFIRE level 5, while the lowest SNR obtained by SAFIRE level 3 combined with iterative beam hardening correction (iBHC).

#### 4.5 CNRs Values

The mean value of contrast to noise ratios was 2.90, 2.35, and 1.94 for SAFIRE s5, SAFIRE s3, and FBP respectively (Figure 9). CNRs of SAFIRE reconstructions were higher compared with FBP and CNRs with SAFIRE s5 were significantly higher compared with FBP ( $p < 0.05$ ). On the other hand, when the iBHC algorithm was used, the CNRs decreased from high to low levels for all reconstruction techniques. In SAFIRE level 5, the CNRs increased by 67% with the use of iBHC reconstructions compared to FBP ( $p < 0.05$ ). The reduction in noise levels was mainly responsible for the increase in SNRs and CNRs for both SAFIRE level 3 and level 5.

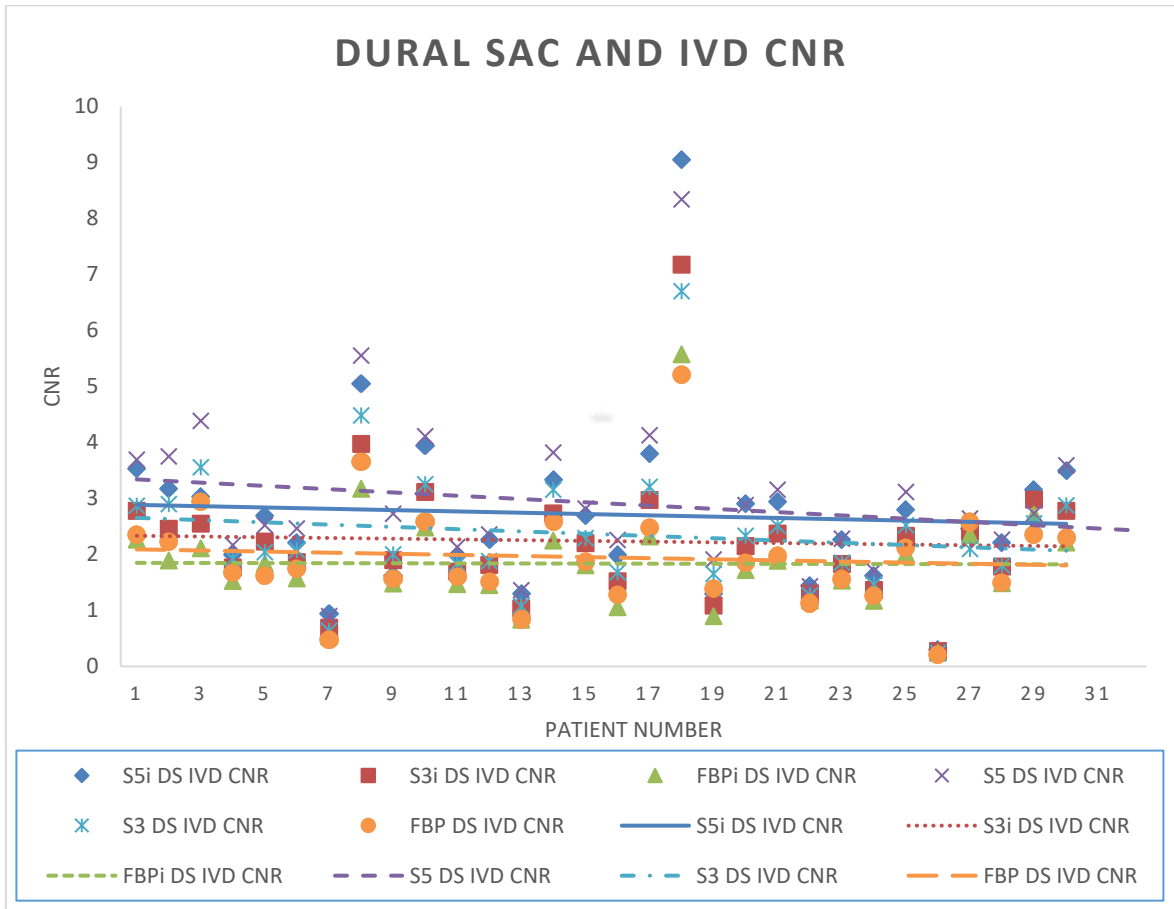


Figure 9 The influence of 6 types of reconstruction algorithms on CNR of the Dural sac region the highest contrast to noise ratio (CNR) obtained by SAFIRE level 5, while the lowest CNR obtained by filtered back projection (FBP) combined with iterative beam hardening correction (iBHC).

#### 4.6 SNR as a Function of Patient BMI

Figure 10 show that with or without iBHC algorithm, SAFIRE level 5 was most successful in enhancing the overall SNR of the dural sac. The overall SNR was slightly higher for SAFIRE s5 alone. The relationship between SNRs improvement showed a non-linear fashion with BMI. The higher SNR values improvement by SAFIRE s5 were 17.7, 15.45, and 10 for BMI values of 25, 32, and 31 kg./m<sup>2</sup> respectively. On the other hand, the lowest SNR improvement values were 0.07, 0.17, and 0.22 for BMI values of 29, 26, and 40 kg./m<sup>2</sup>.

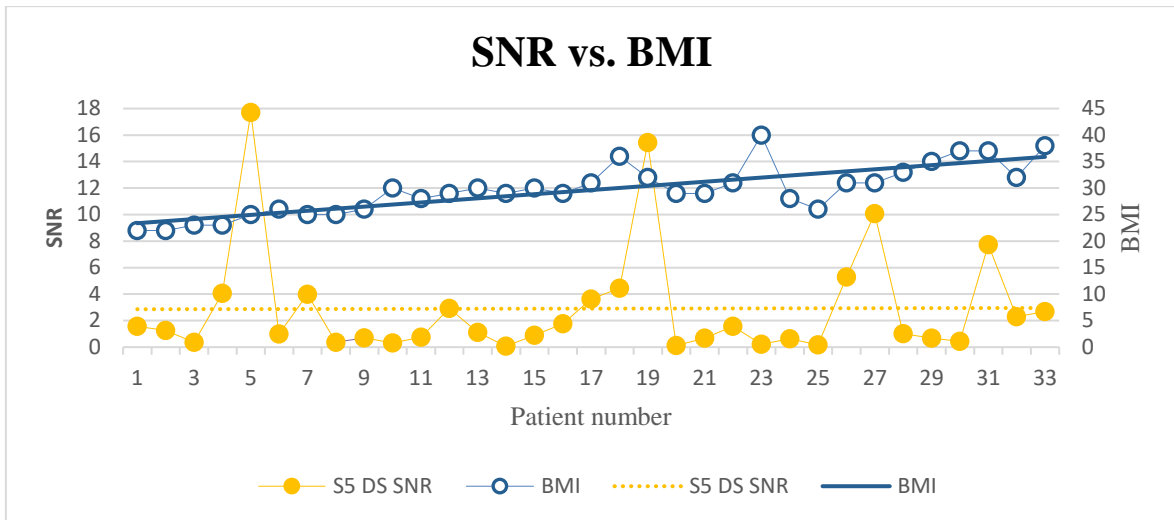


Figure 10 The influence of SAFIRE level 5 reconstruction algorithms on SNR as a function of BMI, the SNR trend line without slope while the BMI trend line with positive slope.

#### 4.7 CNR as a Function of Patient BMI

SAFIRE level 5 was most successful in enhancing the overall CNR of the dural sac. The mean value of CNR improvement value was 2.69 when iBHC was used with SAFIRE s5 (Figure 11). However, the combination between iBHC and SAFIRE level 5 had the most CNR improvement value (9.06) for a patient with a BMI of 31 kg./m<sup>2</sup>, the overall CNR was slightly higher for SAFIRE s5 alone. The correlation between CNRs improvement showed a non-linear fashion according to BMI. The higher CNR values improvement by SAFIRE s5 were 8.34, and 5.56 for BMI values of 25, and 36 kg./m<sup>2</sup> respectively. On the other hand, the lowest CNR improvement values were 0.26, and 0.9 for BMI values of 31, and 25 kg./m<sup>2</sup>.



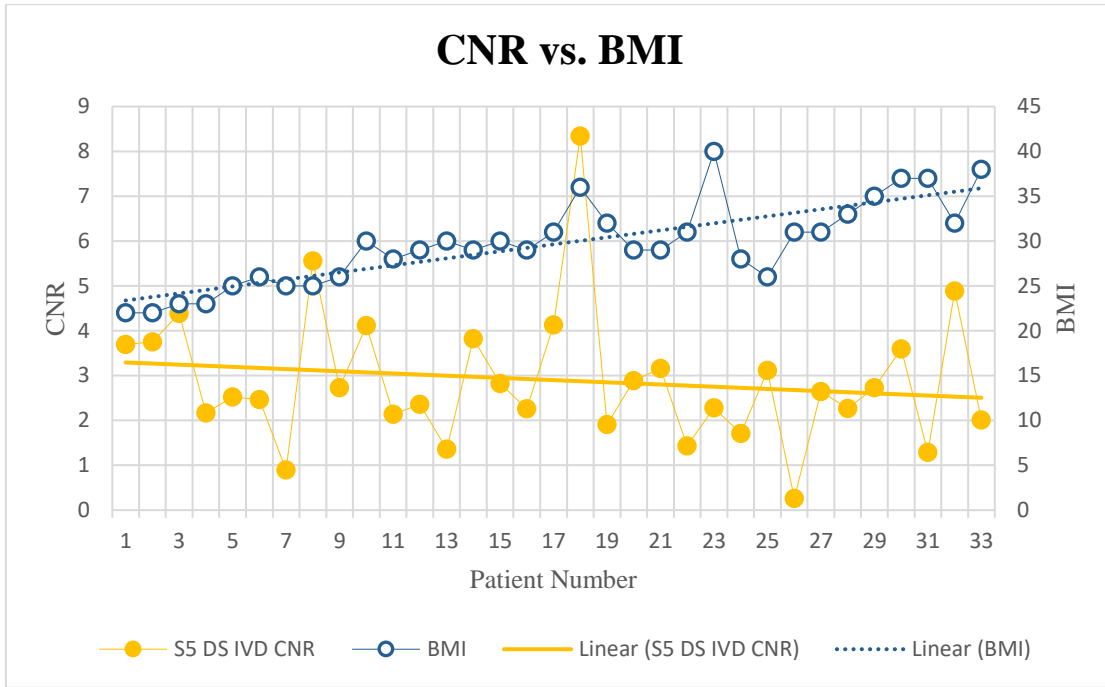


Figure 11 The influence of SAFIRE level 5 reconstruction algorithms on CNR as a function of BMI, the BMI trend line exhibit positive slope while CNR trend line exhibit negative slope, by conclusion we have inverse relationship.

#### 4.8 Effective Dose

Figure 12 shows a strong positive relationship between radiation effective dose and patient BMI  $p < 0.001$ . Based on the data collected from the population, the mean effective dose (ED) for the whole population was 1.9 mSv ranging from (0.69 – 5.96 mSv). The highest effective dose was reported for a female with a BMI of over 35 kg./m<sup>2</sup>., who is 61 years old. The lowest value was reported for a 70 years old female with a BMI of 22 kg./m<sup>2</sup>.

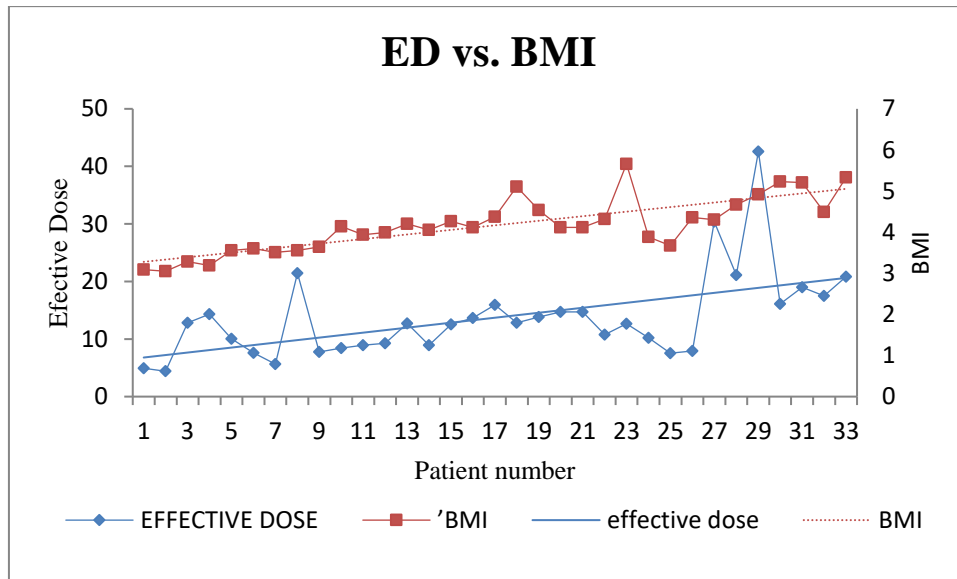


Figure 12 The relationship between radiation effective dose and patient BMI. Both trend line parallel and exhibit positive relationship.

#### 4.9 Qualitative Analysis

The quality of the images from the eight anatomical regions was similar among the observers with good agreement, according to the grading system was based on European standards for computed tomography for the evaluation of disc herniation and lumbar spine (Table 2).

#### 4.10 Discussion

According to our results, using the SAFIRE algorithm, the CT number values for IVD increased from the baseline algorithm (FBP) and were most noted when SAFIRE s5 was used without any significant changes with FBP ( $p= 0.08$ ) or SAFIRE s3 ( $p= 0.09$ ). Also, utilizing the SAFIRE algorithm has no impact or any significant changes ( $p>0.05$ ) on the CT number values for psoas muscle compared to the FBP algorithm. In addition, the mean values for CT numbers for the right psoas muscle region were 54.64, 54.36, and 54.30 for SAFIRE s5, SAFIRE s3, and FBP respectively. Furthermore, using the SAFIRE algorithm has no impact or any significant changes ( $p>0.05$ ) on the CT number values compared to the FBP algorithm. This is because the SAFIRE algorithm is a two-part

process that involves performing various corrections on the raw data to remove artifacts before reducing the noise in the image space. It can improve the image quality and reduce the overall image contrast. The consistency of the mean density values of the data revealed that the algorithm did not affect the image contrast(Seo et al., 2018).

On the other hand, when iBHC was combined with SAFIRE and FBP, CT number values showed significant changes ( $p>0.05$ ). The images reconstructed with FBP integrated with the iBHC algorithm showed an increase in CT number values compared to FBP alone and over both levels of the SAFIRE algorithm without iBHC in all ROIs. This was compared to the values of images reconstructed using the same algorithm without iBHC. The reduction of low-energy photons as they pass through a material is known as the attenuated effect. This phenomenon shifts the energy of the beam as it moves through the material. Based on direct reconstructions of images, iBHC achieves flatness of the final image (Jin et al., 2015).

The combination of the SAFIRE and iBHC provides a smaller absolute mean and variance than the iBHC. Algorithms such as IR, IR-BHC, and FBP all produce equal attenuation coefficients. On the other hand, the iBHC method exhibits a bias in the reconstructed values. This is most likely due to the presence of high-density objects in the data set(Jin et al., 2015). IR-BHC method is more effective at reducing the number of streaking artifacts while preserving the edges' shape and uniform regions. The difference between the ground truth and the reconstruction also shows how effective IR-BHC is in removing these artifacts. In the low attenuation region, the accuracy of the three methods is roughly equal. Although various methods produce lower accuracy density estimates in the high attenuation regions, the IR-BHC algorithm is the most accurate. This method also produces clearer and more accurate structures(Jin et al., 2015).

SAFIRE had a good impact in reducing noise values in the IVD region, psoas muscle, and dural sac and was most effective when using SAFIRE level 5. SAFIRE s5 had a significant noise reduction compared to SAFIRE s3 and FBP ( $p<0.05$ ). For more than four decades, medical scanners have been using the traditional FBP methods to reconstruct images. The use of this technology has been attributed to its accuracy and computational efficiency. FBP can't handle noise properly as it fails to model the non-ideal behaviors of the CT system, especially from decreased dose like fundamental properties of X-ray physics (e.g., beam hardening and scatter), the statistical nature of the data acquisition

(e.g., limited X-ray photon flux and electronic noise), and geometric factors of the system (e.g., partial volume or finite X-ray focal spot size and detector cell size)(Mohammadinejad et al., 2021). Also, for the FBP method, the standard deviation is reduced as the inverse square root of the  $CTDI_{vol}$  is conserved (Ghetti et al., 2013).

While IR typically performs an image reconstruction by optimizing an objective function, which is iteratively performed between the projection space and the image space. It usually models the computed tomography system, detection process, and x-ray attenuation using the known object information to reduce edge-preserving noise(Mohammadinejad et al., 2021).IR methods offer many advantages over the traditional FBP, such as better modeling of the CT system and the x-ray spectrum. In addition, photon statistics can be used to improve the accuracy of reconstructions by reducing the artifacts and improving the dose efficiency. To minimize the noise and improve the transparency of the image, information such as the object's detail in local regions can be included. Furthermore, IR algorithms can handle irregular scanning even if the data acquisition does follow a different geometry (Mohammadinejad et al., 2021).

The reduction of the noise in iterative reconstruction is increased with the SAFIRE strength being applied proportionally (Ghetti et al., 2013). The noise texture and level of noise reduction will vary depending on the strength of the reconstruction. For instance, strength 1 is noisier, while strength 5 is smoother. A study has been conducted on the use of low-dose CT scanning and SAFIRE to diagnose lumbar disc herniation. It revealed that the image quality of the combined scan and examination was no different from that of the routine dose. In addition, the clinical diagnosis results were also good. Compared to routine-dose scanning. In addition, the clinical diagnosis results were good (Booz et al., 2019).

Although the SAFIRE algorithm reduces the noise values, it showed a negative effect when combined with iBHC and make worse. For instance, when combined with the iBHC algorithm, noise values increased for FBP, SAFIRE s3, and SAFIRE s5. This can be explained according to how the iBHC algorithm works. The iBHC is a raw data-based method that can improve the quality of images by reducing the artifacts produced by beam hardening. It utilizes 3D forward projection and a two-compartment model to maintain anatomical structures while reducing the overall beam hardening artifacts. The initial condition for optimization is the reconstruction of the FBP (Siemens Medical Solutions

USA, 2013). Also, The iBHC method can suppress some of the streakings, but it is still noticeable due to the dark band connecting the two insertions. This is because the method introduces a bias in the reconstruction.

The SAFIRE algorithm was able to improve the overall SNR and make the dural sac clear again. The mean SNR improvements were 2.9, and 2.2 for SAFIRE s5 and s3 respectively in comparison with the reference SNR value (1.6) for FBP. Also, CNRs of SAFIRE reconstructions were higher compared with FBP, and CNRs with SAFIRE s5 were significantly higher compared with FBP ( $p < 0.05$ ). While reducing the dose required to achieve an acceptable noise level, using SAFIRE can still preserve the image quality and minimize the impact of the algorithm on the overall noise. The consistency of the mean density values showed that the SAFIRE algorithm did not affect the image contrast and decrease the noise values which lead to an increase in the overall SNR values. With SAFIRE, the noise models are set up differently for each strength level, and the stronger the noise reduction target, the more accurate the approximations are (Willeminck et al., 2013),(Miéville et al., 2013). Compared to standard CT scans, the images produced by low-dose IR (level 3 and level 5) scans are more accurate and provide a superior reproduction of various anatomical structures. Some of the anatomical structures that were better reproduced with IR include the trabecular bone, the intervertebral joints, the disks, and the paravertebral muscles (Alshamari et al., 2017). In previous patient studies, iterative reconstruction has been shown to improve the quality of images in terms of CNR and SNR(Scharf et al., 2017).

Concerning iBHC, the Overall SNR was slightly higher for SAFIRE s5 alone (2.9) than for images that combined SAFIRE s5 and iBHC (2.8). Also, the integration between iBHC and FBP had no impact on FBP images alone. Furthermore, when the iBHC algorithm was used, the CNRs decreased from high to low levels for all reconstruction techniques. In SAFIRE level 5, the CNRs increased by 67% with the use of iBHC reconstructions compared to FBP ( $p < 0.05$ ). Although, SAFIRE-iBHC shows a more uniform error map as no high-density objects in the data set, so no bias in the reconstructed values. iBHC achieves flatness of the final image and led to an increased attenuation coefficient. As it removes low frequency reduces overall SNR and increases noise (Siemens Medical Solutions USA, 2013). In addition, the reduction in noise levels was

mainly responsible for the increase in SNRs and CNRs for both SAFIRE level 3 and level 5 according to equation 3.

The body's BMI, which is a measure of weight, is used to determine the amount of fat that a person has which was calculated as follows:  $BMI = \text{weight (kg)} / (\text{height (m)})^2$  (Nuttall, 2015). SAFIRE level 5 was most successful in enhancing the overall SNR and CNR values of the dural sac. The overall SNR and CNR were slightly higher for SAFIRE s5 alone. The relationship between SNRs and CNRs improvement showed a non-linear fashion with BMI. The level of noise reduction and texture that can be achieved through the SAFIRE algorithm will vary depending on the strength that was used for each reconstruction. Through two iterative correction loops, the algorithm can remove image artifacts before reducing the noise in the image space (Seo et al., 2018). Compared to the full-dose FBP images, the use of SAFIRE at lower doses resulted in better and similar results. The improvement in image quality is less for obese patients or those with heavy weights (>75kg) (Scharf et al., 2017).

The mean effective dose was 1.9 mSv ranging from (0.69 – 5.96) mSv. The highest ED value was 5.96mSv, belonging to female aged 61 years with a BMI of 35 kg. /m<sup>2</sup>. While the lowest value achieved calculated is 0.69mSv belonging to a female whose 70 years old with a BMI of 22 kg. /m<sup>2</sup>. (Figure 12) shows a strong positive relationship between radiation effective dose and patient BMI  $p < 0.001$ . The value of effective dose varies from patient to patient ranging from 0.69 to 5.96 mSv. The maximum effective dose for any patient of 5.96 mSv was found for a 61 years old female with a BMI of 35 kg/m<sup>2</sup>, and a weight of 98 kg. The higher dose was mainly due to the presence of sensory organs in the scanning range, which is why it was most effective for a female patient. The World Health Organization has classified over 70% of patients as overweight or obese (Nuttall, 2015).

Effective dose is also a function of patient body parameters. Statistical analysis of this relationship was performed and shows a strong positive relationship between radiation effective dose and patient BMI  $p < 0.001$ . The study revealed that an increase in BMI was associated with a higher radiation dose that was obtained from a QCT using an automatic tube current modulation system. This type of system is commonly used by MDCT scanners

to adjust the radiation dose depending on the patient's attenuation. It is designed to maintain diagnostic image quality while reducing the overall radiation dose. (C. H. Lee et al., 2008).

In addition, the automated tube current modulation technique can also lead to higher radiation doses for patients who are obese. This is because the higher the beam attenuation, the more noise it can cause and the need for a higher current to maintain the image quality (Kalra et al., 2004). A previous study revealed that the radiation used during body CT examinations is significantly higher in patients who are heavier than 100 kilograms while using automated tube current modulation. They receive an organ dose that is typically twice as high as that of those of 60 kilograms (Israel et al., 2010). Another study claimed that for every kilogram of weight, the effective dose of radiation increased by 0.13 mSv. For instance, if a person's BMI goes up by 5 kg/m<sup>2</sup>, the increase in effective dose would be 1.95 mSv. Although the reasons for this increase may be multi-factorial, it has been shown that the amount of intra-abdominal fat and periumbilical fat can have a significant effect on the radiation dose (Chan et al., 2012). Although there was no difference between men and women in this study, women had higher intra-abdominal fat levels, which could be associated with a higher dose (Chan et al., 2012).

The grading system was based on European standards for computed tomography for the evaluation of disc herniation and lumbar spine. The quality of the images from the eight anatomical regions was similar among the observers with good agreement. The QCT with the lowest dose values and reconstructed with SAFIRE level 5 compared to that of standard high dose, do not have a negative impact on the image quality. There was no significant difference in the detection of pathology between the QCT and standard protocols. However, the reviewers considered some criteria such as visually sharp reproduction of the perithecial fat, intervertebral radicular canals, nerve roots, and reproduction of the paravertebral ligaments to be visualized more clearly and were more certain of their findings with standard high-dose CT. The current study has shown that low-dose CT improves visualization of most anatomical structures as well as gives observers higher confidence in evaluating some common pathologic lesions compared with standard high-dose CT. Pathology was more clearly seen with low-dose CT and the reviewers were more certain of their findings. Even though these benign lesions are of no clinical concern, the easier detection with CT may reflect the benefit of using low-dose CT

to visualize small lesions in general, including metastases. Further research on the evaluation of the diagnostic accuracy of low-dose CT is warranted, especially for the detection of lesions that are highly dependent on visualization of cortical or trabecular bone such as fracture detection. On QCT, the spinal canal area was more narrowed compared to axial cuts. This finding is explained by the ability of multidetector CT and using of a low kVp setting, which discriminates between soft tissues and cortical bone (Eun et al., 2012). CT also shows excellent osseous dimensions of canals and posterior elements(Eun et al., 2012). It can also distinguish the degenerative changes in the joints, as well as the spondylolysis and erosive changes in the facet orientation and the zygapophyseal joints(Wassenaar et al., 2012).



## Chapter 5

This chapter shows the conclusion of the study and its limitations.

### 5.1 Conclusion

The use of QCT and using SAFIRE level 5 resulted in higher SNR, CNR, and fewer noise values compared to classic FBP and other levels of SAFIRE. Also, QCT using SAFIRE level 5 revealed equivalent image quality compared to standard protocols of the lumbar spine CT. The adjustment of the algorithms' strength according to BMI using the tube modulation technique is required. This imaging technique is ideal for patients who are not suitable for magnetic resonance imaging.

### 5.2 Limitations

The quality of images produced by low-dose CT scans is not always the same as those produced by standard CT scans. Also, the accuracy of these scans needs to be studied in a larger population. Despite the high level of interobserver agreement, further studies are needed to confirm the accuracy of these scans. Although the use of certain image quality criteria such as CT numbers and noise levels is usually appropriate for monitoring the nature of the noise, further measurements of the modulation transfer function and the noise power spectrum are also needed to gain a deeper understanding of the noise.

## References

- Alshamari, M., Geijer, M., Norrman, E., & Geijer, H. (2014). Low-dose computed tomography of the lumbar spine: A phantom study on imaging parameters and image quality. *Acta Radiologica*, *55*(7), 824–832. <https://doi.org/10.1177/0284185113509615>
- Alshamari, M., Geijer, M., Norrman, E., Lidén, M., Krauss, W., Jendeberg, J., Magnuson, A., & Geijer, H. (2017). Impact of iterative reconstruction on image quality of low-dose CT of the lumbar spine. *Acta Radiologica*, *58*(6), 702–709. <https://doi.org/10.1177/0284185116669870>
- Alshamari, M., Geijer, M., Norrman, E., Lidén, M., Krauss, W., Wilamowski, F., & Geijer, H. (2016). Low dose CT of the lumbar spine compared with radiography: A study on image quality with implications for clinical practice. *Acta Radiologica*, *57*(5), 602–611. <https://doi.org/10.1177/0284185115595667>
- Andersen, H. K., Völgyes, D., & Martinsen, A. C. T. (2018). Image quality with iterative reconstruction techniques in CT of the lungs—A phantom study. *European Journal of Radiology Open*, *5*(February), 35–40. <https://doi.org/10.1016/j.ejro.2018.02.002>
- Arjah, Hamza, Hjouj, M. (2020). *Low Dose Brain CT, Comparative Study With Brain Post Processing Algorithm* [Al-Quds university]. <https://dspace.alquds.edu/handle/20.500.12213/5272>
- Arjah, H., Hjouj, M., & Hjouj, F. (2019). Low dose brain CT, comparative study with brain post processing algorithm. *ACM International Conference Proceeding Series*, 1–7. <https://doi.org/10.1145/3379299.3379308>
- Booz, C., Nöske, J., Martin, S. S., Albrecht, M. H., Yel, I., Lenga, L., Gruber-Rouh, T., Eichler, K., D'Angelo, T., Vogl, T. J., & Wichmann, J. L. (2019). Virtual noncalcium dual-energy CT: Detection of lumbar disk herniation in comparison with standard gray-scale CT. *Radiology*, *290*(3), 446–455. <https://doi.org/10.1148/radiol.2018181286>
- Chan, V. O., McDermott, S., Buckley, O., Allen, S., Casey, M., O'Laoide, R., & Torreggiani, W. C. (2012). The relationship of body mass index and abdominal fat on the radiation dose received during routine computed tomographic imaging of the abdomen and pelvis. *Canadian Association of Radiologists Journal*, *63*(4), 260–266. <https://doi.org/10.1016/j.carj.2011.02.006>
- Chou, R., Qaseem, A., Owens, D. K., & Shekelle, P. (2011). Diagnostic imaging for low back pain: Advice for high-value health care from the American college of physicians. *Annals of Internal Medicine*, *154*(3), 181–189. <https://doi.org/10.7326/0003-4819-154-3-201102010-00008>
- Dieleman, J. L., Baral, R., Birger, M., Bui, A. L., Bulchis, A., Chapin, A., Hamavid, H., Horst, C., Johnson, E. K., Joseph, J., Lavado, R., Lomsadze, L., Reynolds, A., Squires, E., Campbell, M., DeCenso, B., Dicker, D., Flaxman, A. D., Gabert, R., ... Murray, C. J. L. (2016). US spending on personal health care and public health, 1996-2013. *JAMA - Journal of the American Medical Association*, *316*(24), 2627–2646. <https://doi.org/10.1001/jama.2016.16885>
- Eun, S. S., Lee, H. Y., Lee, S. H., Kim, K. H., & Liu, W. C. (2012). MRI versus CT for the diagnosis of lumbar spinal stenosis. *Journal of Neuroradiology*, *39*(2), 104–109. <https://doi.org/10.1016/j.neurad.2011.02.008>
- European Guidelines for DECT. (2004). European Guidelines on Quality Criteria for Computed Tomography European Guidelines on Quality Criteria. *Eur J Radiol*, *50*, 1–71.
- Fleischmann, D., & Boas, F. E. (2011). Computed tomography—old ideas and new technology. *European Radiology*, *21*(3), 510–517. <https://doi.org/10.1007/s00330-011-2056-z>
- Gervaise, A., Osemont, B., Lecocq, S., Noel, A., Micard, E., Felblinger, J., & Blum, A. (2012). CT image quality improvement using adaptive iterative dose reduction with wide-volume acquisition on 320-detector CT. *European Radiology*, *22*(2), 295–301. <https://doi.org/10.1007/s00330-011-2271-7>
- Ghetti, C., Palleri, F., Serreli, G., Ortenzia, O., & Ruffini, L. (2013). Physical characterization of a new ct iterative reconstruction method operating in sinogram space. *Journal of Applied Clinical Medical Physics*, *14*(4), 263–271. <https://doi.org/10.1120/jacmp.v14i4.4347>

- Godt, J. C., Johansen, C. K., Martinsen, A. C. T., Schulz, A., Brøgger, H. M., Jensen, K., Stray-Pedersen, A., & Dormagen, J. B. (2021). Iterative reconstruction improves image quality and reduces radiation dose in trauma protocols; A human cadaver study. *Acta Radiologica Open*, 10(10), 20584601211055389. <https://doi.org/10.1177/20584601211055389>
- Grant, K., & Raupach, R. (2012). SAFIRE : Sinogram Affirmed Iterative Reconstruction. *Technical Report*, 1–8.
- Hamza, A., Osman, N. D., Ahmad, M. Z., Hussein, M., & Aziz, M. E. (2022). Assessment of effective dose and nonlinear transformation algorithm for low dose brain computed tomography. *Radiography*, 28, S2. <https://doi.org/10.1016/j.radi.2022.10.019>
- Hara, A. K., Paden, R. G., Silva, A. C., Kujak, J. L., Lawder, H. J., & Pavlicek, W. (2009). Iterative reconstruction technique for reducing body radiation dose at CT: Feasibility study. *American Journal of Roentgenology*, 193(3), 764–771. <https://doi.org/10.2214/AJR.09.2397>
- Hoeffner, E. G., Mukherji, S. K., Srinivasan, A., & Quint, D. J. (2012). Neuroradiology back to the future: Spine imaging. *American Journal of Neuroradiology*, 33(6), 999–1006. <https://doi.org/10.3174/ajnr.A3129>
- Israel, G. M., Cicchiello, L., Brink, J., & Huda, W. (2010). Patient size and radiation exposure in thoracic, pelvic, and abdominal CT examinations performed with automatic exposure control. *American Journal of Roentgenology*, 195(6), 1342–1346. <https://doi.org/10.2214/AJR.09.3331>
- Jarvik, J. G., & Deyo, R. A. (2002). *Diagnostic Evaluation of Low Back Pain with Emphasis on Imaging Purpose: To review evidence on the diagnostic accuracy of clinical information and imaging for patients with low back pain in primary care settings.*
- Jin, P., Bouman, C. A., & Sauer, K. D. (2015). A Model-Based Image Reconstruction Algorithm With Simultaneous Beam Hardening Correction for X-Ray CT. *IEEE Transactions on Computational Imaging*, 1(3), 200–216. <https://doi.org/10.1109/tci.2015.2461492>
- Kalra, M. K., Maher, M. M., Toth, T. L., Kamath, R. S., Halpern, E. F., & Saini, S. (2004). Comparison of z-axis automatic tube current modulation technique with fixed tube current CT scanning of abdomen and pelvis. *Radiology*, 232(2), 347–353. <https://doi.org/10.1148/radiol.2322031304>
- Komlosi, P., Zhang, Y., Leiva-Salinas, C., Ornan, D., Patrie, J. T., Xin, W., Grady, D., & Wintermark, M. (2014). Adaptive statistical iterative reconstruction reduces patient radiation dose in neuroradiology CT studies. *Neuroradiology*, 56(3), 187–193. <https://doi.org/10.1007/s00234-013-1313-z>
- Lee, C. H., Goo, J. M., Lee, H. J., Ye, S. J., Park, C. M., Chun, E. J., & Im, J. G. (2008). Radiation dose modulation techniques in the multidetector CT era: From basics to practice. *Radiographics*, 28(5), 1451–1459. <https://doi.org/10.1148/rg.285075075>
- Lee, S. H., Yun, S. J., Jo, H. H., Kim, D. H., Song, J. G., & Park, Y. S. (2018). Diagnostic accuracy of low-dose versus ultra-low-dose CT for lumbar disc disease and facet joint osteoarthritis in patients with low back pain with MRI correlation. *Skeletal Radiology*, 47(4), 491–504. <https://doi.org/10.1007/s00256-017-2811-6>
- Lee, T. Y., & Chhem, R. K. (2010). Impact of new technologies on dose reduction in CT. *European Journal of Radiology*, 76(1), 28–35. <https://doi.org/10.1016/j.ejrad.2010.06.036>
- Lurie, J. D. (2005). What diagnostic tests are useful for low back pain? *Best Practice and Research: Clinical Rheumatology*, 19(4), 557–575. <https://doi.org/10.1016/j.berh.2005.03.004>
- McCollough, C. H., Chen, G. H., Kalender, W., Leng, S., Samei, E., Taguchi, K., Wang, G., Yu, L., & Pettigrew, R. I. (2012). Achieving routine submillisievert CT scanning: Report from the Summit on Management of Radiation Dose in CT. *Radiology*, 264(2), 567–580. <https://doi.org/10.1148/radiol.12112265>
- Mehta, S. R. et al. (2015). Reduced Lung-Cancer Mortality with Low-Dose Computed Tomographic Screening. *New England Journal of Medicine*, 687–696.

- Mehta, D., Thompson, R., Morton, T., Dhanantwari, A., Shefer, E., & Healthcare, P. (2013). ITERATIVE MODEL RECONSTRUCTION : SIMULTANEOUSLY LOWERED COMPUTED TOMOGRAPHY RADIATION DOSE AND IMPROVED IMAGE QUALITY. *MEDICAL PHYSICS INTERNATIONAL Journal*, 1–9.
- Miéville, F. A., Gudinchet, F., Brunelle, F., Bochud, F. O., & Verdun, F. R. (2013). Iterative reconstruction methods in two different MDCT scanners: Physical metrics and 4-alternative forced-choice detectability experiments - A phantom approach. *Physica Medica*, 29(1), 99–110. <https://doi.org/10.1016/j.ejmp.2011.12.004>
- Mohammadinejad, P., Mileto, A., Yu, L., Leng, S., Guimaraes, L. S., Missert, A. D., Jensen, C. T., Gong, H., McCollough, C. H., & Fletcher, J. G. (2021). Ct noise-reduction methods for lower-dose scanning: Strengths and weaknesses of iterative reconstruction algorithms and new techniques. *Radiographics*, 41(5), 1493–1508. <https://doi.org/10.1148/rg.2021200196>
- Niemann, T., Kollmann, T., & Bongartz, G. (2008). Diagnostic performance of low-dose CT for the detection of urolithiasis: A meta-analysis. *American Journal of Roentgenology*, 191(2), 396–401. <https://doi.org/10.2214/AJR.07.3414>
- Nuttall, F. Q. (2015). Body mass index: Obesity, BMI, and health: A critical review. In *Nutrition Today* (Vol. 50, Issue 3, pp. 117–128). <https://doi.org/10.1097/NT.0000000000000092>
- Omarah, A., Hjouj, M., Aljamal, M., & Hjouj, F. (2022). Metal artifact reduction and iterative reconstruction algorithms in computed tomography imaging of hip prostheses. *Radiography*, 28, S4. <https://doi.org/10.1016/j.radi.2022.10.024>
- Omarah Naser Saed Abd Alqader, M. H. (2021). *Evaluation of the Application of Orthopedic Metal Artifact Reduction and Iterative Reconstruction Algorithms in CT Imaging of Hip Prostheses*. Al-Quds University.
- Omoumi, P., Verdun, F. R., Salah, Y. Ben, Berg, B. C. V., Lecouvet, F. E., Malghem, J., Ott, J. G., Meuli, R., & Becce, F. (2014). Low-dose multidetector computed tomography of the cervical spine: Optimization of iterative reconstruction strength levels. *Acta Radiologica*, 55(3), 335–344. <https://doi.org/10.1177/0284185113494981>
- Oxland, T. R. (2016). Fundamental biomechanics of the spine-What we have learned in the past 25 years and future directions. *Journal of Biomechanics*, 49(6), 817–832. <https://doi.org/10.1016/j.jbiomech.2015.10.035>
- Park, C. K., Lee, H. J., & Ryu, K. S. (2017). Comparison of root images between post-myelographic computed tomography and magnetic resonance imaging in patients with lumbar radiculopathy. *Journal of Korean Neurosurgical Society*, 60(5), 540–549. <https://doi.org/10.3340/jkns.2016.0809.008>
- Plichta, S. B., & Kelvin, E. A. (2021). MUNRO'S Statistical Methods for Health Care Research. In *Nuevos sistemas de comunicación e información*.
- Scharf, M., Brendel, S., Melzer, K., Hentschke, C., May, M., Uder, M., & Lell, M. M. (2017). Image quality, diagnostic accuracy, and potential for radiation dose reduction in thoracoabdominal CT, using Sinogram Affirmed Iterative Reconstruction (SAFIRE) technique in a longitudinal study. *PLoS ONE*, 12(7). <https://doi.org/10.1371/journal.pone.0180302>
- Scheffel, H., Alkadhi, H., Leschka, S., Plass, A., Desbiolles, L., Guber, I., Krauss, T., Gruenenfelder, J., Genoni, M., Luescher, T. F., Marincek, B., & Stolzmann, P. (2008). Low-dose CT coronary angiography in the step-and-shoot mode: Diagnostic performance. *Heart*, 94(9), 1132–1137. <https://doi.org/10.1136/hrt.2008.149971>
- Seo, N., Chung, Y. E., An, C., Choi, J. Y., Park, M. S., & Kim, M. J. (2018). Feasibility of radiation dose reduction with iterative reconstruction in abdominopelvic CT for patients with inappropriate arm positioning. *PLoS ONE*, 13(12). <https://doi.org/10.1371/journal.pone.0209754>
- Shin, H. J., Chung, Y. E., Lee, Y. H., Choi, J. Y., Park, M. S., Kim, M. J., & Kim, K. W. (2013). Radiation dose reduction via sinogram affirmed iterative reconstruction and automatic tube voltage modulation

- (CARE kV) in abdominal CT. *Korean Journal of Radiology*, 14(6), 886–893. <https://doi.org/10.3348/kjr.2013.14.6.886>
- Siemens Medical Solutions USA, I. (2013). *510(K) SUMMARY FOR SOMATOM Force* (Vol. 510).
- Singh, S., Kalra, M. K., Hsieh, J., Licato, P. E., Do, S., Pien, H. H., & Blake, M. A. (2010). Abdominal CT: Comparison of adaptive statistical iterative and filtered back projection reconstruction techniques. *Radiology*, 257(2), 373–383. <https://doi.org/10.1148/radiol.10092212>
- Söderberg, M. (2016). Overview, practical tips and potential pitfalls of using automatic exposure control in CT: Siemens CARE Dose 4D. *Radiation Protection Dosimetry*, 169(1), 84–91. <https://doi.org/10.1093/rpd/ncv459>
- Tang, C., & Aggarwal, R. (2013). Imaging for musculoskeletal problems. *InnovAiT: Education and Inspiration for General Practice*, 6(11), 735–738. <https://doi.org/10.1177/1755738013491081>
- Thrall J. (2012). Radiation exposure in CT scanning and risk: where are we? *Radiology*, 264(2), 325–328.
- Toshiba, M. S. (2012). AIDR 3D Iterative Reconstruction: Integrated, Automated and Adaptive Dose Reduction. *White Paper*, 1–10.
- Venkatesan, M., Fong, A., & Sell, P. J. (2012). CT scanning reduces the risk of missing a fracture of the thoracolumbar spine. *The Journal of Bone and Joint Surgery. British Volume*, 94-B(8), 1097–1100. <https://doi.org/10.1302/0301-620x.94b8.29397>
- Warncke, M. L., Wiese, N. J., Tahir, E., Sehner, S., Heinemann, A., Regier, M., Püschel, K., Adam, G., Weinrich, J. M., & Laqmani, A. (2020). Highly reduced-dose CT of the lumbar spine in a human cadaver model. *PLoS ONE*, 15(10), 1–12. <https://doi.org/10.1371/journal.pone.0240199>
- Wassenaar, M., Van Rijn, R. M., Van Tulder, M. W., Verhagen, A. P., Van Der Windt, D. A. W. M., Koes, B. W., De Boer, M. R., Ginai, A. Z., & Ostelo, R. W. J. G. (2012). Magnetic resonance imaging for diagnosing lumbar spinal pathology in adult patients with low back pain or sciatica: A diagnostic systematic review. *European Spine Journal*, 21(2), 220–227. <https://doi.org/10.1007/s00586-011-2019-8>
- Wassenaar, M., Van Rijn, R. M., Van Tulder, M. W., Verhagen, A. P., Van Der Windt, D. A. W. M., Koes, B. W., De Boer, M. R., Ginai, A. Z., & Ostelo, R. W. J. G. (2012). Magnetic resonance imaging for diagnosing lumbar spinal pathology in adult patients with low back pain or sciatica: A diagnostic systematic review. *European Spine Journal*, 21(2), 220–227. <https://doi.org/10.1007/s00586-011-2019-8>
- Weinrich, J. M., Well, L., Regier, M., Behzadi, C., Sehner, S., Adam, G., & Laqmani, A. (2018). MDCT in suspected lumbar spine fracture: comparison of standard and reduced dose settings using iterative reconstruction. *Clinical Radiology*, 73(7), 675.e9–675.e15. <https://doi.org/10.1016/j.crad.2018.02.015>
- Willemink, M. J., De Jong, P. A., Leiner, T., De Heer, L. M., Nievelstein, R. A. J., Budde, R. P. J., & Schilham, A. M. R. (2013a). Iterative reconstruction techniques for computed tomography Part 1: Technical principles. *European Radiology*, 23(6), 1623–1631. <https://doi.org/10.1007/s00330-012-2765-y>
- Willemink, M. J., De Jong, P. A., Leiner, T., De Heer, L. M., Nievelstein, R. A. J., Budde, R. P. J., & Schilham, A. M. R. (2013b). Iterative reconstruction techniques for computed tomography Part 1: Technical principles. *European Radiology*, 23(6), 1623–1631. <https://doi.org/10.1007/s00330-012-2765-y>
- Winklehner, A., Karlo, C., Puippe, G., Schmidt, B., Flohr, T., Goetti, R., Pfammatter, T., Frauenfelder, T., & Alkadhi, H. (2011). Raw data-based iterative reconstruction in body CTA: Evaluation of radiation dose saving potential. *European Radiology*, 21(12), 2521–2526. <https://doi.org/10.1007/s00330-011-2227-y>
- Wurdeman, S. R., Stevens, P. M., Campbell, J. H., Davie-Smith, F., Coulter, E., Kennon, B., Wyke, S., Paul, L., Ingegneria, F., Magistrale, L., Di, M., In, S., Resistive, M., Della, R., Bekrater-Bodmann, R., Daniel E Shumer, N. J. N. P. S., & Nagla, dr madhu. (2017). 乳鼠心肌提取 HHS Public Access. *Physiology & Behavior*, 176(5), 498–503. <https://doi.org/10.2214/AJR.12.8986> Model-Based

- Yang, C. H., Wu, T. H., Chiou, Y. Y., Hung, S. C., Lin, C. J., Chen, Y. C., Sheu, M. H., Guo, W. Y., & Chiu, C. F. (2014). Imaging quality and diagnostic reliability of low-dose computed tomography lumbar spine for evaluating patients with spinal disorders. *Spine Journal*, *14*(11), 2682–2690. <https://doi.org/10.1016/j.spinee.2014.03.007>
- Zhao, Y., & Li, M. (2015). Iterative beam hardening correction for multi-material objects. *PLoS ONE*, *10*(12), 1–13. <https://doi.org/10.1371/journal.pone.0144607>
- Zheng, K., Wen, Z., & Li, D. (2021). The Clinical Diagnostic Value of Lumbar Intervertebral Disc Herniation Based on MRI Images. *Journal of Healthcare Engineering*, 2021. <https://doi.org/10.1155/2021/5594920>

# Ethical Approval

Al-Quds University  
Jerusalem  
Deanship of Scientific Research



جامعة القدس  
القدس  
عمادة البحث العلمي

Research Ethics Committee  
Committee's Decision Letter

Date: October 9, 2022  
Ref No: 250/REC/2022

Dears Dr. Mohammad Hjouj, Mr. Israa Jamal Odeh,

Thank you for submitting your application for research ethics approval. After reviewing your application entitled "Influence of Iterative Reconstruction Algorithm on Image Quality of Low-Dose Lumbar Spine CT" the Research Ethics Committee confirms that your application is in accordance with the research ethics guidelines at Al-Quds University.

We would appreciate receiving a copy of your final research report/ publication.

Thank you again and wish you a productive research that serves the best interests of your subjects.

PS: This letter will be valid for two years.

Sincerely,

Suheir Ereqat, PhD  
Associate Professor of Molecular Biology

Research Ethics Committee Chair

Cc. Prof. Imad Abu Kishek - President  
Cc. Members of the committee  
Cc. file

Abu-Dies, Jerusalem P.O.Box 20002  
Tel-Fax: #970-02-2791293

[research@admin.alquds.edu](mailto:research@admin.alquds.edu)

أبوديس، القدس ص.ب. 20002  
تلفاكس: #970-02-2791293

## تأثير خوارزمية إعادة البناء التكراري على جودة الصورة في التصوير المقطعي المحوسب بجرعة منخفضة جدًا للعمود الفقري القطني

إعداد: إسراء عودة

إشراف: د. محمد الحجوج

### الملخص

التصوير المقطعي الكمي (QCT) أو قياس الكثافة هو فحص جديد في التصوير المقطعي المحوسب (CT) المستخدم لتشخيص كثافة المعادن في العظام. مسح QCT هو بروتوكول جرعة منخفضة بقيمة جرعة فعالة تبلغ 1 مللي سيفرت (mSv). تؤدي تقنية تقليل الجرعة إلى انخفاض كبير في الجرعة الفعالة على حساب جودة الصورة حيث تستخدم طريقة الإسقاط الخلفي المفلتر التقليدي (FBP). تهدف هذه الدراسة إلى تقييم تأثير خوارزمية الأشعة تحت الحمراء على جودة الصورة وقياس الجرعة الفعالة من بروتوكول QCT لجرعة منخفضة من التصوير المقطعي المحوسب للعمود الفقري القطني. تكونت هذه الدراسة من 33 مريضاً من كلا الجنسين الذين اشتبه سريرياً في إصابتهم بالأم أسفل الظهر وهشاشة العظام خلال الفترة من 7 يوليو 2021 حتى تاريخ الموافقة الأخلاقية. تم تطبيق أنواع مختلفة من الخوارزميات ، الإسقاط الخلفي المفلتر (FBP) ، إعادة البناء التكراري المؤكد (SAFIRE) ، وتصحيح تصلب الحزمة التكرارية (iBHC). كانت معايير جودة الصورة عبارة عن رقم CT والضوضاء والإشارة وتم تحليلها بواسطة ثلاث مناطق ذات أهمية (ROIs). تمثل RIOs الثلاثة التشريح التالي (القرص الفقري ، العضلة القطنية اليمنى ، والكيس الجداري) على التوالي من المنطقة 1 - المنطقة 3. بالإضافة إلى ذلك ، من أجل التحليل النوعي ، تمت مقارنة الصور التي أعيد بناؤها بواسطة SAFIRE s5 مع نظام الدرجات وفقاً للمعايير الأوروبية لـ CT لـ تقييم فتق القرص والعمود الفقري. أظهرت النتائج الملحوظة لنسبة الإشارة إلى الضوضاء (SNR) ونسبة التباين إلى الأنف (CNR) تحسناً للصور عند إعادة بنائها بواسطة مستوى SAFIRE 5 ، بمتوسط SNR يبلغ 2.9 وهو أعلى بكثير من خوارزميات إعادة الإعمار الأخرى ( $p > 0.05$ ). أيضاً ، كان متوسط معدل الوفيات من 2.9 وهو أعلى بكثير من تقنيات إعادة البناء الأخرى ( $p > 0.05$ ). متوسط الجرعة الفعالة لجميع السكان كان 1.9 ملي سيفرت. تمكنت خوارزمية SAFIRE من تقليل مستويات الضوضاء في جميع RIO. كانت جودة الصور وفقاً لنظام الدرجات وفقاً للمعايير الأوروبية للتصوير المقطعي المحوسب لتقييم فتق القرص والعمود الفقري الخشبي متشابهة بين المراقبين مع اتفاق جيد. لا توجد علاقة بين مؤشر كتلة الجسم و SNR و CNR و الجرعة الفعالة. في الختام ، أدى استخدام QCT واستخدام مستوى SAFIRE 5 إلى ارتفاع SNR و CNR وقيم ضوضاء أقل مقارنةً بـ FBP الكلاسيكي ومستويات SAFIRE الأخرى. أيضاً ، كشف QCT باستخدام مستوى SAFIRE 5 عن جودة صورة مكافئة مقارنة بالبروتوكولات القياسية للتصوير المقطعي المحوسب للعمود الفقري القطني.